Recent Developments on Optical Aptasensors for the Detection of Pro-Inflammatory Cytokines with Advanced Nanostructures

Kathrine Nygaard Borg, Yi-ping Ho, Shuwen Zeng

WILEY-VCH

Title: Recent developments on optical aptasensors for the detection of pro-inflammatory cytokines with advanced nanostructures

*Kathrine Nygaard Borg, Yi-Ping Ho, and Shuwen Zeng**

K.N. Borg

Department of Biomedical Engineering, The Chinese University of Hong Kong, Shatin, Hong Kong SAR, China.

Y.-P. Ho

Department of Biomedical Engineering, The Chinese University of Hong Kong, Shatin, Hong Kong SAR, China.

Centre for Biomaterials, The Chinese University of Hong Kong, Hong Kong SAR, China.

Hong Kong Branch of CAS Center for Excellence in Animal Evolution and Genetics, Hong Kong SAR, China.

State Key Laboratory of Marine Pollution, City University of Hong Kong, Hong Kong SAR, China.

S. Zeng

Laboratory of Light, Nanomaterials & Nanotechnologies (L2n), CNRS-UMR 7076, Université de Technologie de Troyes, 10000, Troyes, France

Email: shuwen.zeng@cnrs.fr

Keywords: aptamers, cytokines, optical biosensors, aptasensors, gold nanoparticles

In the realm of immune response, pro-inflammatory cytokines play a crucial role in regulating various physiological functions. Accurate measurement of these low-molecular-weight proteins is essential for understanding immune function, predicting diseases, and monitoring treatment effects. Optical aptasensors with advanced nanostructures, which utilize aptamers as bio-probes, have emerged as a promising technology for cytokine detection, offering advantages over traditional antibody-based nanobiosensors. Aptamers, single-stranded nucleic acids with high specificity and affinity, enable cost-effective mass production and consistent quality. Optical biosensors incorporating aptamers exhibit stability, resistance to environmental factors, and prolonged functionality. This review explores the current methodologies and advancements in optical aptasensors for cytokine detection, highlighting their potential as robust tools in diagnostics, and therapeutics. Specifically, the applications of surface plasmon resonance (SPR) and fluorescence techniques in aptasensors are discussed, focusing on the innovative approaches used to enhance sensitivity and specificity in cytokine detection. Notable examples of aptasensor designs utilizing nanoparticles, Förster resonance energy transfer (FRET), and amplification strategies are presented. These designs demonstrate high affinity, specificity, and improved sensitivity in detecting pro-inflammatory cytokines such as interferon gamma (IFN-γ). Overall, optical aptasensors show great promise in advancing our understanding of cytokine-related disorders and enabling effective interventions.

1. Introduction

In the intricate landscape of immune responses, cytokines, low-molecular-weight proteins, stand as pivotal orchestrators, regulating inflammation, homeostasis, and various physiological functions.[1] These signalling molecules, secreted by immune cells, govern cell-to-cell communication and influence crucial processes like cell replication, apoptosis, and disease progression.[2] Disruption of this delicate balance can lead to severe consequences, as seen in the "cytokine storm," associated with diseases like avian flu, SARS, and COVID-19.[3-6]

Beyond immune regulation, comprehensive reviews highlight the impact of cytokines on diverse aspects of biology and medicine.[7-10] The dynamic nature of cytokine secretion poses challenges in accurate measurement, crucial for understanding immune function, predicting diseases, and monitoring treatment effects. This discussion dives into published works on optical biosensors for cytokines, that provide solutions to challenges such as low concentrations and interference, enabling rapid and precise detection using high affinity bio-receptors. An advantageous aspect of optical sensors lies in their ability to directly convert molecular binding

events or biological reactions into a quantifiable signal, proportionate to the concentration of analyte molecules.

While antibodies are commonly adopted as receptors in optical biosensors, their high cost and storage difficulties pose inherent challenges inhibiting their widespread use. Drawing inspiration from the success of antibody-based sensing, DNA-based bio-receptors are gaining increasing interest. Aptamers, characterized by their single-stranded nucleic acid structure spanning 15–40 nucleotides, offer a stable tertiary configuration that facilitates high-affinity and specific binding to target molecules.[11-13] The Systematic Evolution of Ligands by Exponential Enrichment (SELEX), introduced in 1990, underpins aptamer discovery.[14] SELEX involves iteratively enriching nucleic acid libraries by selectively amplifying sequences that bind to target molecules, employing techniques such as polymerase chain reaction (PCR) or reverse transcription-polymerase chain reaction (RT-PCR).[15] This method yields aptamers with exceptional specificity and affinity. Aptamers offer a versatile and precise approach for optical biosensing, particularly in the detection of small molecules like cytokines.[8, 16, 17]

Expanding on the advantages of aptamers over antibodies, the transition towards optical aptasensors represents a paradigm shift in biosensor technology. Aptamers, with their smaller size and facile modification, offer cost-effective mass production, a critical edge over antibodies. Optical biosensors, incorporating aptamers as bio-probes, capitalize on their stability, resistance to environmental factors, and prolonged functionality, overcoming limitations seen in traditional immunosensors sensitive to pH, temperature, and shelf-life constraints.[18-22]

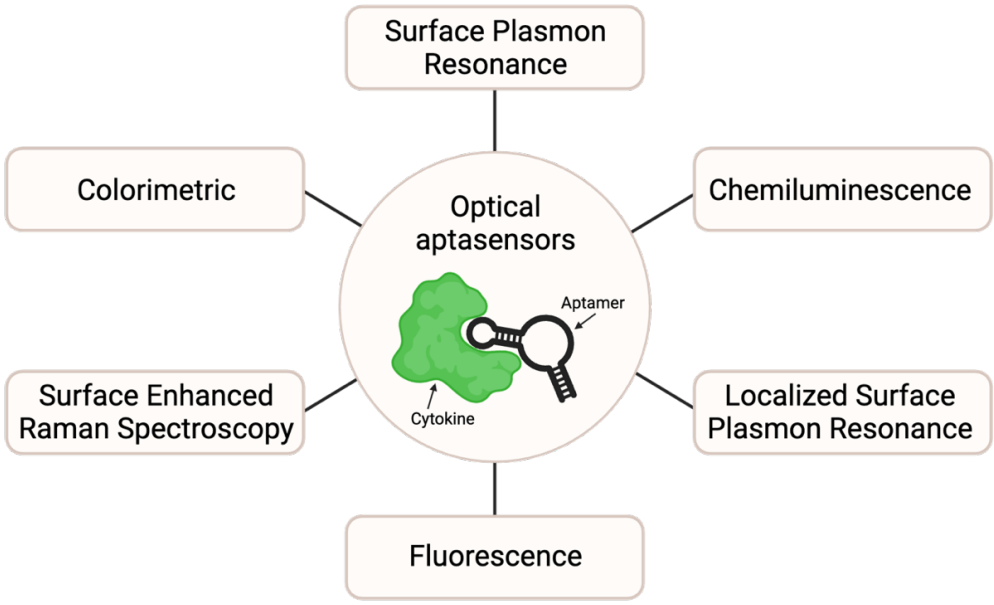

Figure 1. Overview of the different types of optical aptasensors covered in this review.

While immunosensors using antibodies remain prevalent, ongoing research focuses on aptasensors to circumvent challenges associated with antibody-based biosensors, especially in cytokine detection. Despite inherent challenges related to specificity and affinity, ongoing research aims to enhance the performance of optical aptasensors, including the use of nanoparticles for heightened sensitivity and colorimetric readouts for point-of-care tests.[23-25] This review comprehensively examines current methodologies and advancements from the past five years, with a few older studies included as notable examples (**Figure 1**), providing insights into the evolving landscape of aptasensor technology for cytokine detection for diagnostics, therapeutics, and screening.

2. Surface Plasmon Resonance and Localized Surface Plasmon Resonance

Surface plasmon resonance (SPR) biosensors, being the most predominant and extensively applied technique, offer high sensitivity, robustness, cost-effectiveness, and multiplexing capabilities. Within SPR biosensors, two main approaches are employed: standard SPR and localized surface plasmon resonance (LSPR). These methods differ in the location of the resonance phenomenon, occurring on thin metallic films or metal nanoparticles, respectively.[26]

SPR is defined by the presence of an evanescent wave field, generated at the interface by total internal reflection, extending approximately 100 nm from the surface of a metallic film.[27] In standard SPR biosensors, alterations in the refractive index near the planar metal sensor surface are detected when target molecules bind to immobilized recognition elements, leading to changes in the resonance angle of surface plasmon waves.[27] On the other hand, LSPR involves the real-time recognition of surface-bound analyte molecules through shifts in photon absorption and scattering characteristics of conduction-band electrons localized on the surfaces of metallic nanoparticles.[26] Both SPR and LSPR biosensors offer label-free sensing, simplifying experimental procedures, avoiding potential labelling interference, and enabling real-time monitoring of bindings events. Changes from bioreceptor-analyte binding events, brought by target-induced structural changes or competitive binding leading to strand displacement, cause detectable changes in the resonance angle or wavelength in SPR and LSPR, respectively.[28-30]

Yet, for cytokine detection, both SPR and LSPR biosensors encounter challenges in detecting low-concentration molecules, with detection limits approaching 10 pg mL^{-1}. To overcome this limitation, the utilization of aptamers as recognition elements presents a compelling solution due to their small size and higher analyte-probe mass ratio. A recent advancement in this direction proposed a two-site binding detection method utilizing an aptamer-antibody sandwich-based approach for the simultaneous detection of cardiac disease biomarkers, here among tumor necrosis

factor-alpha (TNF-α, ~17.3 kDa).[31] To facilitate multiplexing, the authors fabricated a mixed aptamer chip featuring aptamer sequences specific to N-terminal pro-brain natriuretic peptide (NT-proBNP) and TNF-α. Upon analyte binding, the chip was exposed to corresponding analyte-specific antibodies for signal amplification (**Figure 2A**). In deciding whether the surface-immobilized capture receptor should be the aptamer or antibody, the Langmuir isotherm was employed to estimate the adsorption coefficient (K_{ads}). Notably, for the aptamers, the binding strength toward their target surpassed that of the antibody by almost two-fold, as exemplified by the TNF-α specific aptamer in **Figure 2B (i)** and the anti-TNF-α antibody in **Figure 2C**. Thus, the aptamer was selected as the capture probe, while the antibody served as detection probe in the sandwich complex. For effective multiplexing, the aptamers against the NT-proBNP and TNF-α were immobilized on the surface via EDC/NHC binding chemistry in a 1:1 ratio. This approach, however, led to a 2-fold reduction of the binding constant (**Figure 2B [ii]**), ascribed to the dilution of aptamer binding sites and potential steric hindrance arising from the use of two distinct aptamer structures. The binding properties of aptamers have been correlated with their surface density, particularly impacting the kinetic association constant. A decrease in surface concentration has been observed to enhance affinity, likely due to the increased free space facilitating conformational changes upon target binding,[32] however this is likely also related to target size as it may be the determining factor of the steric hindrance.[33] Consequently, enhanced sensitivity might be compromised if the SPR substrate is fully saturated, while also aiming to detect larger biomolecules. The utilization of two structurally different aptamers, as adapted by Lee et al., could exacerbate the impact of substrate saturation on binding affinity and the related detection sensitivity.[31] However, by adapting the sandwich sensing mode an increased detection sensitivity of NT-proBNP and TNF-α was achieved, as observed in **Figure 2D** where various TNF-α concentrations ([i] 0.5 pM, [ii] 1.5 pM, [iii] 2.5 pM, [iv] 4 pM, and [v] 10 pM) was detected using an anti-TNF-α antibody for signal enhancement (**Figure 2E**).

In addition to hybrid sandwich structures like aptamer-antibody combinations, the application of two aptamers alone has been explored for amplified detection. For instance, the coupling of a streptavidin aptamer with an interferon gamma (IFN-γ) aptamer has demonstrated the ability to detect IFN-γ (~17 kDa) at concentrations as low as 0.03 and 0.01 nM.[30, 34] In both studies, the binding event between IFN-γ and the immobilized IFN-γ specific aptamer induced a structural change facilitating recognition by streptavidin molecules, thereby amplifying the biosensor response.[30, 34] Concerns about steric hindrances in such an aptamer complex were addressed with varying probe concentrations and spacers between the two aptamers in complex. The authors found

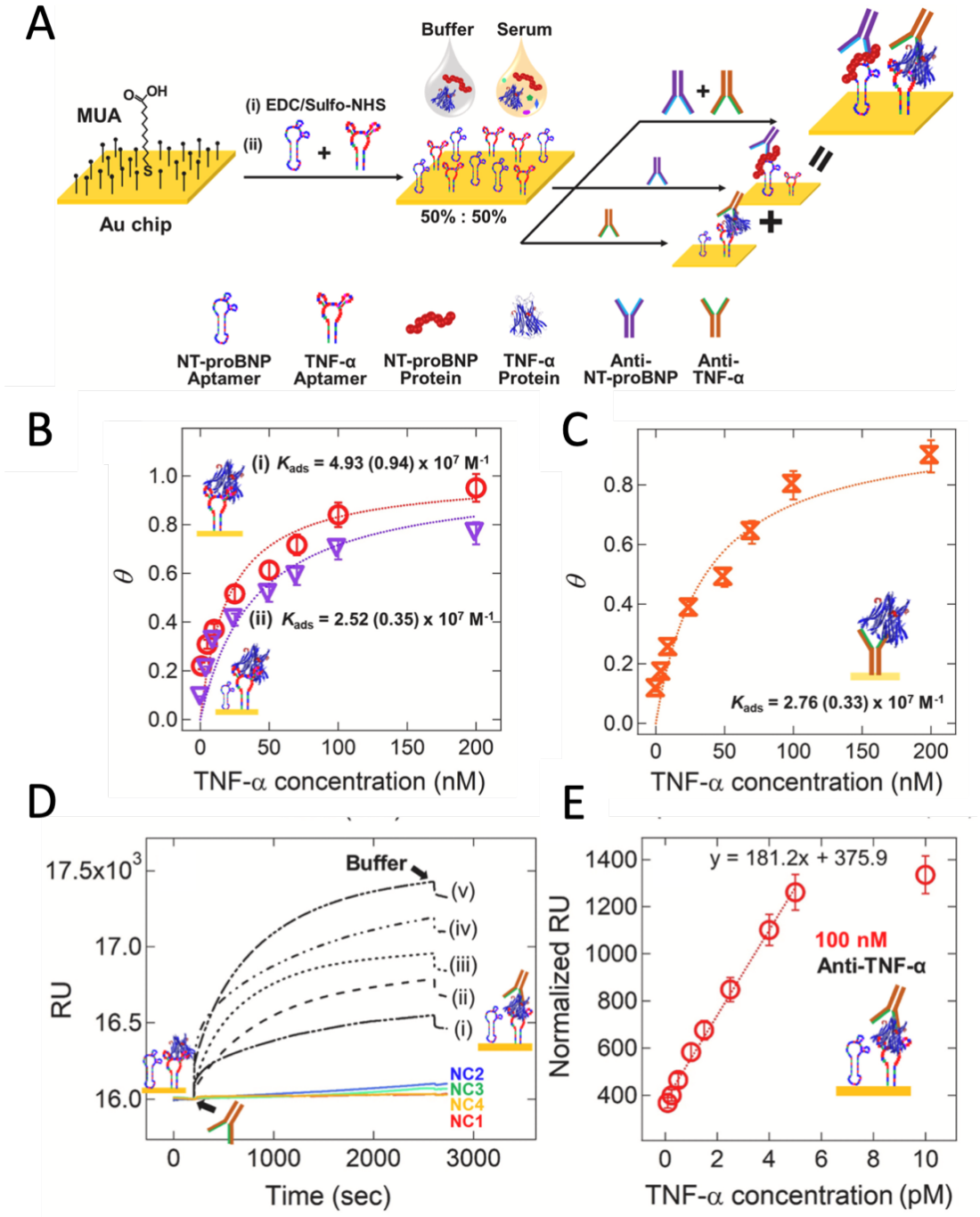

Figure 2. Simultaneous detection of cardiac disease biomarkers on mixed aptamer-chip by SPR. (**A**) Scheme of the strategy for simultaneous detection of NT-proBNP and TNF-α. Specific recognition of NT-proBNP and TNF-α on chip surface modified with 1:1 mixed aptamers with subsequent binding of anti-NT-proBNP and/or anti-TNF-α antibodies. (**B**) Langmuir adsorption isotherm plot of fractional surface coverage (theta) on gold chip composed of 100 % TNF-α aptamer and (**C**) 100 % anti-TNF-α antibody. (**D**) Real-time SPR response for adsorption of different concentrations of TNF-α onto mixed NT-proBNP:TNF-α aptamer monolayer at a ratio of 1:1 followed by exposure to 100 nM anti-TNF-α antibody and (**E**) corresponding plot of normalized RU values from SPR curves at various TNF-α concentrations. Reproduced with permission.[31] Copyright 2023, Elsevier B.V.

that intermediate probe concentration (500 nM) and a 12-mer spacer suggested optimal biosensor response.[30] Despite achieving a 4-fold enhanced sensor response with streptavidin-aptamer binding, as reported by Chang and co-workers,[30] it is important to note that Lee et al.'s dual specificity[31], utilizing both target-specific aptamers and antibodies for detection, is not attainable with streptavidin alone due to its inability to differentiate between different aptamer complexes. Moreover, Lee et al. demonstrated precise detection with robust sensitivity of the cardiac disease biomarkers in both buffer and human blood samples spiked with NT-proBNP and/or TNF-α. However, the authors acknowledged non-specific adsorption during the simultaneous analysis, reflected in increased differences in normalized refractive unit values for mixed versus individual proteins.[31] To address this common SPR issue, particularly for gold-based sensors due to their reactivity, antifouling strategies in aptamer-based SPR sensors often include blocking agents such as polyethylene glycol (PEG).[35] Notably, a binary self-assembled monolayer (SAM) with antifouling properties, comprising two frequently employed thiol molecules, 3,6-dioxa-8-mercaptooctan-1-ol (DMOL) and 11-mercaptoundecanoic acid (11-MUA), exhibited enhanced selectivity compared to surfaces lacking antifouling modifications.[36] However, the exploration into different antifouling strategies for aptamer-based SPR sensors for cytokines is very limited. Moreover, the potential offered by nano-structural designs of the sensor surfaces has been overlooked. For instance, in immuno-based SPR sensing strategies, the use of a 2D nanomaterial comprising a 1-nm thin $Ge_2Sb_2Te_5$ (GST) layer on either gold or silver nanofilms has demonstrated remarkably ultralow detection limits for TNF-α. These limits reach sub-attomole and sub-femtomolar values, attributed to the high absorption coefficient of the GST layer that enhances the zero-reflection dip, resulting in topological phase singularity.[37, 38] Graphene materials are also gaining increased interest for the use in biosensors, specifically graphene oxide (GO) sheets have been exploited due to its high sensitivity and easy synthesis procedure. An LOD of 1.15 pM for human chorionic gonadotropin (hCG, ~ 36 kDa) was reached utilizing carboxyl-functionalized GO-based SPR with peptide aptamers for strong and high affinity binding.[39]

Recent advancements in nanofabrication have also facilitated the integration of LSPR-based technologies in cytokine detection with aptamer bioreceptors. In LSPR designs, the high analyte-to-probe mass ratio offered by aptamers becomes essential in improving the theoretical limits of LSPR techniques. An exemplary case involves the application of an antibody-derived peptide aptamer (ADPA) designed for interleukin 6 (IL-6, ~20.9 kDa) detection using LSPR imaging (LSPRi).[40] The ADPA, formed by combining three complementarity-determining region (CDR) loops of an anti-IL-6 antibody with minimalist linkers (**Figure 3A**), demonstrated reduced

molecular weight (~3 kDa) and lower mass ratio to cytokines compared to the native antibody. Immobilization of the ADPAs onto a bare gold sensor surface through Au-S bonding enabled the

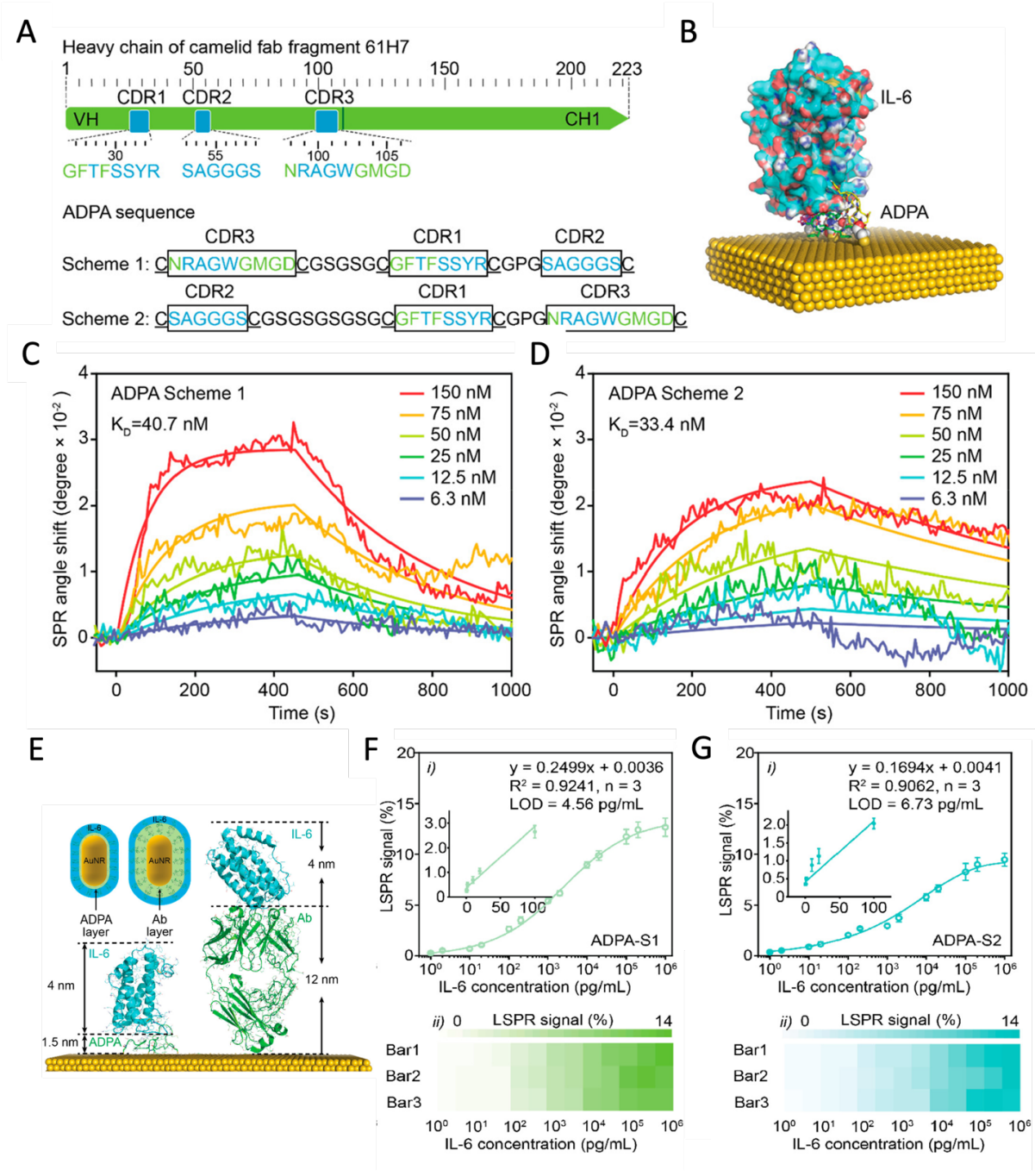

Figure 3. ADPA-based sensing of IL-6. (**A**) CDR-loops adopted from anti-IL-6 antibody and resulting sequences of ADPA scheme 1 and 2. (**B**) Structure of ADPA-IL-6 complex on a gold surface. (**C**) SPR sensorgram of ADPA scheme 1. (**D**) SPR sensorgram of ADPA scheme 2. (**E**) Illustration of IL-6 capture by ADPA (left) and antibody (right) on bare gold surface as well as visualization of receptor layer on AuNR for LSPR sensing. (**F**) Calibration curve of ADPA scheme 1 and (**G**) ADPA scheme 2 LSPRi immunoassay. Reproduced with permission.[40] Copyright 2022, American Chemical Society.

measurement of affinity and kinetic parameters using standard SPR (**Figure 3B**). Despite slightly weaker affinity compared to the native antibody, the ADPA schemes remained comparable to other anti-IL-6 antibodies with K_D values of 40.7 and 33.4 nM (**Figure 3C** and **3D**). For LSPR sensing, the ADPAs were immobilized onto hexadecyltrimethylammonium bromide-capped gold nanorods (CTAB-AuNRs) through Au-S chemistry. This resulted in a plasmonic response increase with thinner recognition layers compared to antibody coating, enabling IL-6 binding closer to the CTAB-AuNR surface (**Figure 3E**). The ADPA-LSPR assay exhibited a LOD of 4.6 pg mL^{-1} for ADPA scheme 1 (**Figure 3F**) and 6.7 pg mL^{-1} for ADPA scheme 2 (**Figure 3G**), showing an 8-fold improvement over the antibody-based LSPR assay (37.4 pg mL^{-1}). The dynamic range spanned approximately six orders of magnitude, from 1 to 5×10^6 pg mL^{-1}, using the ADPA-LSPR immunoassay. In vitro validation of the ADPA-LSPR immunoassay was conducted in blood samples from COVID-19 patients, with or without immunomodulatory treatment (tocilizumab), providing valuable insights into the IL-6 profiles of SARS-CoV-2 inflammation. Interestingly, the authors used cysteine residues for the site-specific direct immobilization of the ADPAs onto the CTAB-AuNRs, differing from the commonly utilized EDC/NHS coupling for antibodies. This alternative approach mitigates disoriented immobilization risks, preserving antigen binding sites and maintaining assay sensitivity. Moreover, conjugating aptamers to nanoparticles may influence their affinity towards targets, particularly as one of the ends of the aptamer becomes immobilized. For instance, He et al. proposed that the decreased affinity observed with the ADPA schemes relative to the native antibody might be attributed, in part, to interactions between amino acids in the CDR regions and the gold surface through Au-nitrogen interactions, leading to unexpected folding of the CDRs.[40, 41] Lin and co-workers also investigated the impact of immobilizing AuNRs at either 3' or 5' end of an aptamer-complement DNA complex on the LSPR refractive index.[42] Previous studies suggested that signal amplification was more pronounced when metallic nanoparticles were in close proximity to the LSPR substrates.[43-45] However, in this study, the initial step involved target binding to surface-immobilized aptamers, followed by the introduction of AuNRs carrying complement DNA which hybridized to unreacted aptamers. Consequently, a higher target concentration resulted in fewer AuNRs binding, leading to a less significant LSPR shift. Utilizing the spectral shift of AuNRs instead of the target allowed the detection of low molecular weight molecules that would otherwise induce a minimal shift, enhancing assay sensitivity. In this case, careful attention should be paid to the competitive binding that occurs between target and the complement DNA on the AuNRs, as this ultimately determines the sensitivity of the assay. Lin et al. also reported issues with the unspecific adsorption of AuNRs to the surface, impacting sensor regeneration. Unspecific adsorption might affect the aptamer

configuration and its affinity towards the target, as aptamer affinity depends on their three-dimensional configurations. To achieve optimal 3D functionality, linkers or spacer may be incorporated to distance the aptamer sequence from the functional modification and immobilization surface, as explored by Chang and co-workers in their SPR setup.[30, 46]

The covered approaches capitalize on the distinct advantages offered by SPR and LSPR techniques, including label-free, compactness, and rapid detection of cytokines, as well as the unique capability to delve into binding affinity, association, and dissociation constants between aptamers and cytokines. In a field where limited characterization techniques extend beyond mere binding affinity assessment, SPR biosensing emerges as a potent tool with the potential to revolutionize aptamer characterization and detection. While SPR has been employed to investigate thermodynamics in protein-peptide interactions,[47] the application of such in-depth explorations to cytokine-aptamer interactions remains an exciting frontier waiting to be further unravelled. Also, while offering promising outcomes in cytokine detection, both SPR and LSPR biosensors employing aptamers have yet to thoroughly investigate the implications of altered binding affinities upon immobilization onto planar substrates or nanoparticles and delve deeper into diverse nanofabrication procedures to enhance detection sensitivities. The general scarcity of studies on aptamer-based SPR and LSPR detection of cytokines is likely attributed to the challenges associated with sensitivity and selectivity, requiring meticulous investigations for optimization.

3. Surface-enhanced Raman Spectroscopy

Surface-enhanced Raman spectroscopy (SERS) is a potent analytical technique rooted in the phenomenon of Raman scattering, a process involving the scattering of light while losing or gaining energy. Specifically, SERS intensifies the detection and identification of minute quantities of target materials by significantly enhancing Raman signals. This enhancement occurs when molecules are adsorbed on or near metallic nanostructures, leading to increased Raman scattering signals in the order of 10^6-10^9 times.[23, 48, 49] The exceptional attributes of SERS, including ultra-sensitivity, label-free, and the capacity for precise fingerprint identification, make it an attractive method for delving into the complexities of biological systems and molecular interactions.[24, 50, 51]

Leveraging SERS technology, IL-6 levels were assessed on a gold nanoparticle (AuNP) array functionalized with an IL-6-specific DNA aptamer.[24, 52] The fabrication of AuNP arrays utilized anodic aluminium oxide (AAO) template-assisted electrochemical deposition, resulting in a uniform distribution of hexagonal patterns of AuNPs with diameters of around 53 nm and 44 nm for canonical pores and AuNPs, respectively, along with sub-10 nm nanogaps. Similar to SPR and

LSPR, the surface density of aptamers significantly influences the biosensor's sensitivity by dictating their capacity to assume the appropriate binding configuration. In the context of SERS IL-6 detection, the authors systematically examined various aptamer concentrations on the AuNP arrays to identify the optimal aptamer density, which yielded the most favourable sensor response. Consequently, the highest G and A band intensity ratio was observed at a 40 μM aptamer concentration. The sensor demonstrated consistent performance across a range of IL-6 concentrations (10^{-12}-10^{-7} M), with the aptamer and IL-6 interaction causing a conformational change and a corresponding decrease in A signal at 763 and 963 cm^{-1}. The SERS intensity ratio (I_{660}/I_{736}) exhibited a linear increase with higher IL-6 concentrations and demonstrated specificity when tested against various non-specific proteins, including other cytokines. Also, the authors successfully detected trace amounts of IL-6 (10^{-12}-10^{-7} M) in spiked serum from new-born calves, with an estimated LOD of 0.8 pM. The label-free aptamer-based SERS sensor proposed by Muhammad et al. demonstrates competitive sensitivity levels among similar solid SERS biosensors detecting cytokines.[24] The only exception is a label-free antibody-coupled AuNP SERS scheme, which achieved a greater sensitivity in IL-6 detection (down to 0.04 pM). This dominance may be attributed to the intrinsic SERS fingerprints of the anti-IL-6 antibody, which, due to its smaller size, a change in aptamer configuration is unable to rival.[53]

In addition to label-free approaches, SERS detection strategies may also involve the use of tags or labels to further enhance sensitivity. Huang and colleagues developed a self-calibrating SERS assay for IL-6 detection using Au@MBN@Ag NPs with fluorescent labelling (**Figure 4A**).[54] The sensor surface featured gold cores encapsulated with 4-mercaptobenzonitrile (MBN) and silver shells, with aptamer functionalization achieved through the interaction between silver and a 5'-thiol-modified IL-6-specific aptamer.[52] IL-6 levels were detected using a recognition-release mechanism, where a complementary DNA strand labelled with a fluorophore was employed. The recognition of IL-6 disrupted the aptamer and cyanine-labelled DNA pairing, leading to fluorophore shedding and a decrease in the Cy3 signal. Self-calibration was achieved by incorporating an internal standard molecule (MBN) into the NPs with a signal in the biologically silent Raman region (1800-2800 cm^{-1}). Sensor stability was enhanced through calibration using MBN, exhibiting peaks at 2227 cm^{-1}, against the Cy3 peaks at 1470 cm^{-1} (**Figure 4B**). After optimizing the external silver layer thickness, ssDNA concentration (aptamer and complementary Cy3-DNA), and IL-6 incubation time, a standard curve covering IL-6 concentrations from 10^{-9} mg mL^{-1} to 10^{-4} mg mL^{-1} was generated, demonstrating a linear relationship between 1470 cm^{-1} (Cy3)/2227 cm^{-1} (MBN) against the IL-6 concentrations (**Figure 4C**). The linear regression (R^2) values were 0.961 and 0.856 when calculated from either the intensity ratio (Cy3/MBN) or Cy3

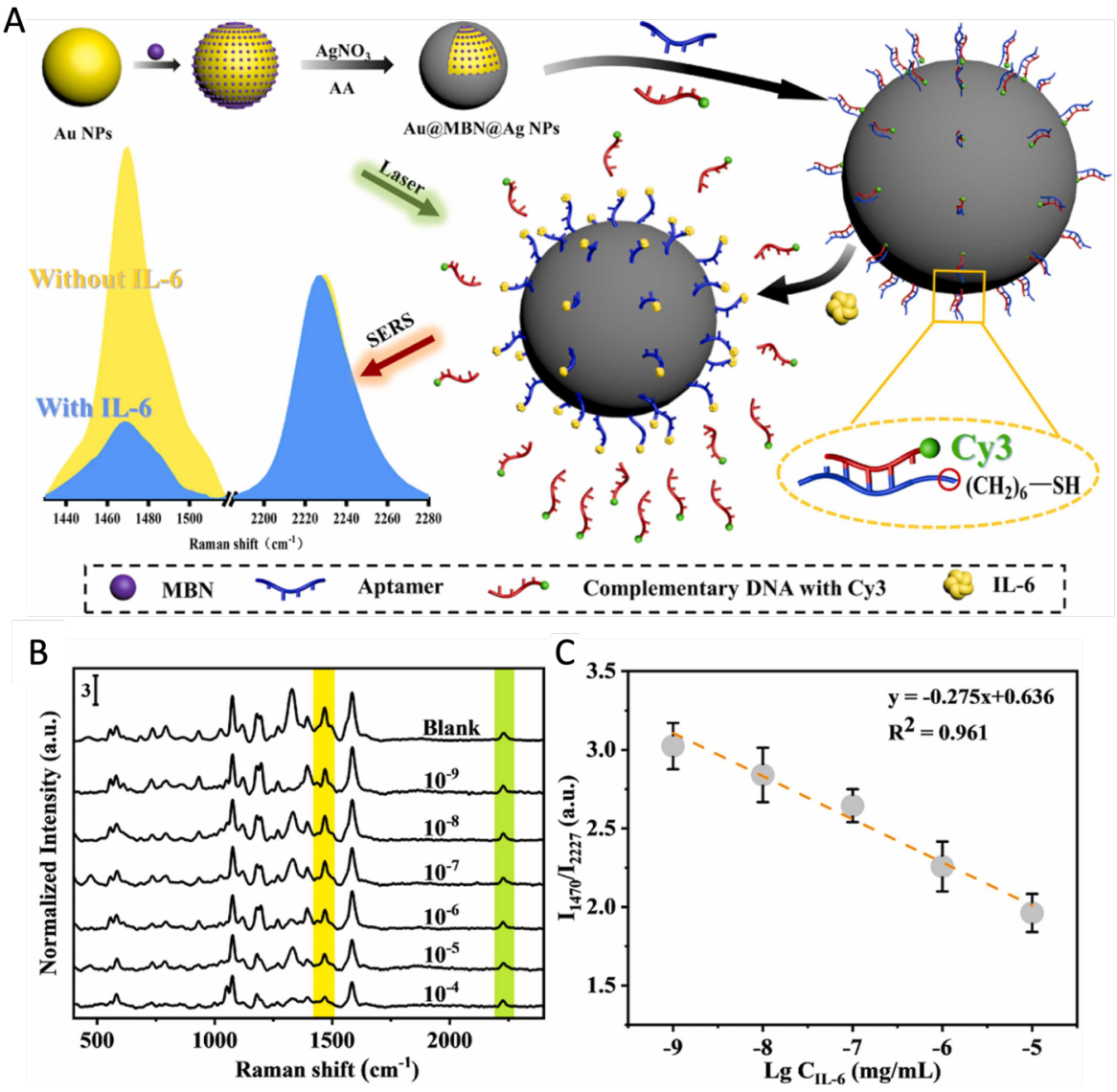

Figure 4. SERS-based self-calibrating aptamer sensor for IL-6 detection. (**A**) Scheme of sensing setup. (**B**) Normalized SERS spectra using Raman intensity at 2227 cm^{-1}. (**C**) The linear relationship between IL-6 concentration and SERS intensity ratio of aptamer sensor. Reproduced with permission.[54] Copyright 2022, Elsevier B.V.

peak intensity, respectively, highlighting the importance of the self-calibrating component. When challenged by interfering substances, the Cy3 signal remained unchanged, showcasing the high specificity of the IL-6-specific aptamer on the NPs.[54] Another label-based SERS sensor employing both antibodies and aptamers complexed with a Raman reporter molecule for TNF-α detection, demonstrated ultralow sensitivity of 0.00437 pg mL^{-1}.[55] However, the assay required a prolonged 2-hour incubation with the target analyte for optimal binding, nearly 1.5-2× longer than the aforementioned SERS sensors. Additionally, an extra step involving magnetic separation of the sandwich immune structures, prolonged the time-to-results. In general, labelled SERS approaches

often offer higher sensitivities but are burdened by the inclusion of the label and may include more specialized experimental procedures with prolonged time-to-results.

The current research in aptameric SERS biosensing of cytokines is relatively sparse; however, innovative use of SERS, as exemplified in this review, highlight its potential for diverse applications. The finely tuned SERS substrates, featuring AuNP arrays and aptamer functionalization, hold promise for expanding SERS applications to detect various cytokines. Additionally, Huang et al.'s development of a self-calibrating SERS assay adds sophistication to the field, emphasizing SERS' adaptability and potential for self-contained, highly precise analytical techniques. Despite these advancements, certain aspects in the application of aptamer-based SERS biosensors, which may enhance their sensitivity, have been neglected. Issues like non-specific binding, observed in prolonged analyte incubations, and the absence of surface blocking by passivating agents such as BSA, as demonstrated by Nie and co-workers, highlight the need for further consideration.[55, 56]

4. Fluorescence

Fluorescence aptasensors have emerged as powerful tools for the sensitive and selective detection of cytokines.[23] In recent studies, researchers have employed diverse strategies to enhance the performance of these aptasensors, ranging from highly specialized nanostructures, label-free sensing, and on/off quenching strategies. These innovative approaches aim to address challenges such as sensitivity, specificity, and practical applicability in complex biological systems.

In continuation of plasmonic sensors utilizing various nanomaterials, nanoparticle-coupling methods in fluorescent sensing stand out for their ability to enable label-free detection. Mahani et al. devised a detection scheme for IL-6 based on Förster resonance energy transfer (FRET) using nitrogen-doped carbon quantum dots (NCD) and AuNPs as a donor-quencher pair.[57] Initially, an IL-6 aptamer (Apt) was linked to the AuNPs via Au-S chemistry. In the absence of the target, the NCDs formed π-π stacking with the Apt-AuNP, leading to significant quenching of the NCD fluorescence. Upon analyte introduction, the aptamer configuration adjusted to bind IL-6, causing the NCDs to dissociate from the AuNPs, thereby restoring their fluorescence. Under standard buffer conditions, the sensor exhibited a linear correlation between emission intensity and IL-6 concentrations within the range of 1.5 to 5.9 pg mL^{-1}, with a calculated LOD of 0.82 pg mL^{-1}. Nevertheless, the authors acknowledge limitations for clinical application, including a restricted detection range that renders it unsuitable for high IL-6 concentrations. Attention must also be paid to the red shift of both excitation and emission wavelengths to mitigate interference from UV absorbers potentially attenuating the fluorescence signal. Various nanoparticle components,

including graphene QDs (GQDs) and QD-aptamer-AuNP complexes, have been utilized for on/off sensing of different cytokines.[58, 59] Moreover, label-free approaches employing luminescent iridium(III) probe and aggregation-induced emission fluorogens (AIEgen) have been developed for simpler detection schemes, with on/off fluorescence regulated by the presence of the cytokine target through structural changes to the aptamer-complexes.[60, 61] Similarly, Xia et al. exploited interfacial reactivity for label-free aptamer-based IFN-γ detection.[62] Analyte binding induced steric hindrance, reducing the reactivity of biotin-labelled aptamers with streptavidin-functionalized interfaces of magnetic beads. When analytes bound to the IFN-γ aptamer, steric hindrance significantly reduced this reactivity. Fluorescent metal-organic frameworks (MOFs) translated this altered interfacial reactivity into a fluorescence-based readout. The method detected IFN-γ within a range of 0.06 fM to 6 pM with an LOD of 0.057 fM. Notably, the aptamer-analyte interaction occurred in solution, minimizing the interference from particle immobilization of the aptamer, and required only a small biotin-label on the aptamer. Additionally, the approach is independent of structure-switching, avoiding sensitivity to assay conditions and tedious optimizations necessary for clinical practice. However, the multi-step process involved in generating fluorescent MOFs renders it a relatively complex sensing strategy. In an alternative nanoparticle-based approach, detection of IL-6 relied on the fluorescent quenching of a FAM-labelled IL-6-specific aptamer upon its adsorption to the surface of a graphene oxide/nickel/platinum nanoparticle micromotor (MM_{GO}).[63] Micromotors (MMs) possess the ability to autonomously move in a solution by converting energy input into motion. Gordón et al. harnessed hydrogen peroxide (H_2O_2) as fuel to propel the $MM_{GO,}$ enabling 'on-the-move' sensing through the recoil force generated by the production of bubbles during the catalysis of H_2O_2, with platinum serving as the catalase. When IL-6 was present, the aptamer's structural change led to separation from the MMs, restoring fluorescence (**Figure 5A**). Successful IL-6 detection was performed in serum samples from infants suspected of sepsis, while achieving an LOD of 0.02 pg mL^{-1} and a linear range covering the clinical levels under optimal conditions (**Figure 5B**). Although the reaction time slightly increased from buffer to serum samples (from 80 μm s^{-1} to 60 μm s^{-1}), the strategy efficiently detected IL-6 in ultra-small volumes (2 μL), despite visible MM aggregation due to magnetism (**Figure 5C**). Recently, this method was optimized for the simultaneous detection of procalcitonin (PCT) and IL-6 using MM_{GO} carrying either PCT-specific or IL-6-specific aptamers, labelled with Alexa405 ($\lambda_{emission}$ = 447 nm) or Alexa488 ($\lambda_{emission}$ = 520 nm), respectively.[64] Overall, MM technology offers advantageous features such as autonomous movement in solution, on-the-move recognition,

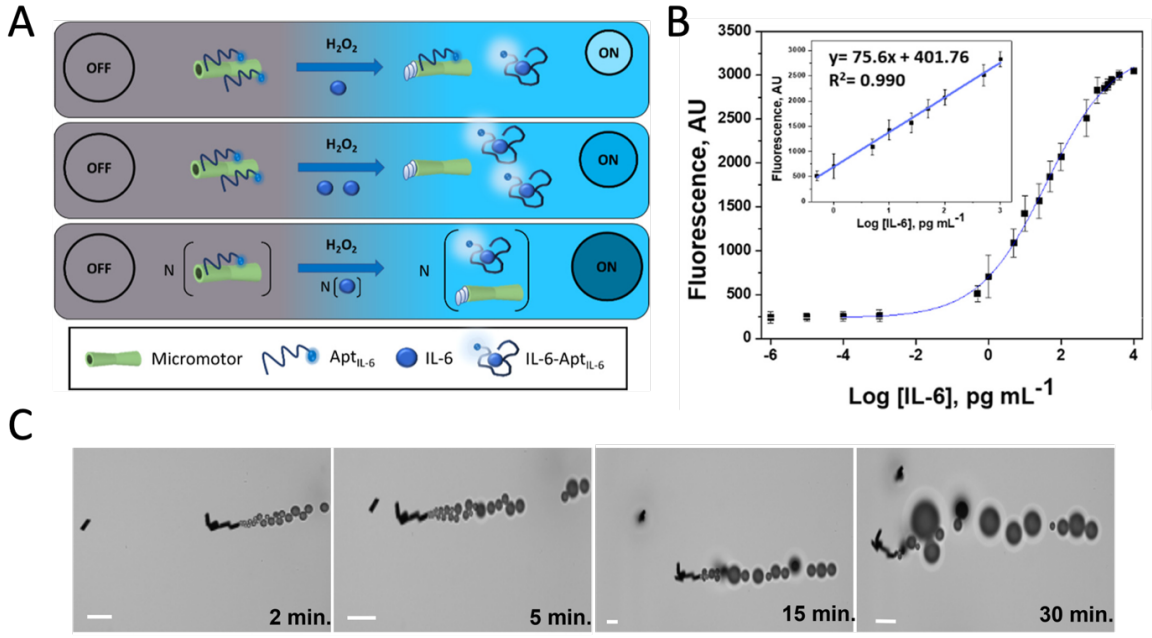

Figure 5. Micromotor strategies for cytokine detection. (**A**) Scheme of MM_{GO}-based assay for IL-6 detection. (**B**) Fluorescence response against various IL-6 concentrations applied in MM_{GO} detection scheme. (**C**) Movement of MMs during time-lapse with aggregation caused by their magnetism. Scale bar: 40 µm. Adapted with permission.[63] Copyright 2022, José Gordón (Licensed under CC BY 4.0).

dynamic analyte search, and improved sensitivity and kinetics. However, the broader application of bubble propulsion MM sensors in biomedical fields is impeded by the potential toxicity of H_2O_2. Alternative MMs based on zinc or magnesium have been suggested, yet, the efficacy of bubble propulsion is significantly influenced by the surrounding medium, necessitating further optimizations.[65]

In another aspect of specialized nanostructures, two-dimensional nanomaterials offer high surface areas for the absorption of bioreceptors, such as ssDNA probes through hydrogen bonding, π-π stacking, and electrostatic interactions.[66, 67] For example, reduced GO (rGO), GO, ReS_2 and TiS_2 nanosheets (NSs) have been utilized for FRET-based or amplified sensing of IFN-γ.[68-70] Recently, cobalt oxyhydroxide (CoOOH) NSs were employed for IFN-γ quantification through a tandem system composed of aptamer, strand displacement amplification (SDA), and CRISPR/Cas12a, referred to as Apt-SCN tandem system.[71] As illustrated in **Figure 6A**, an IFN-γ aptamer forms a duplex with its complementary cDNA. Upon IFN-γ binding, the aptamer releases the cDNA, initiating SDA with a helper DNA (hDNA). As a result, dsDNA products are generated and activate the CRISPR/Cas12a system, leading to cleavage of a long chain FAM-ssDNA probe into short fragments. CoOOH nanosheets readily adsorbs the long probe, quenching the fluorescence via FRET. However, the short fragments are not well adsorbed, resulting in

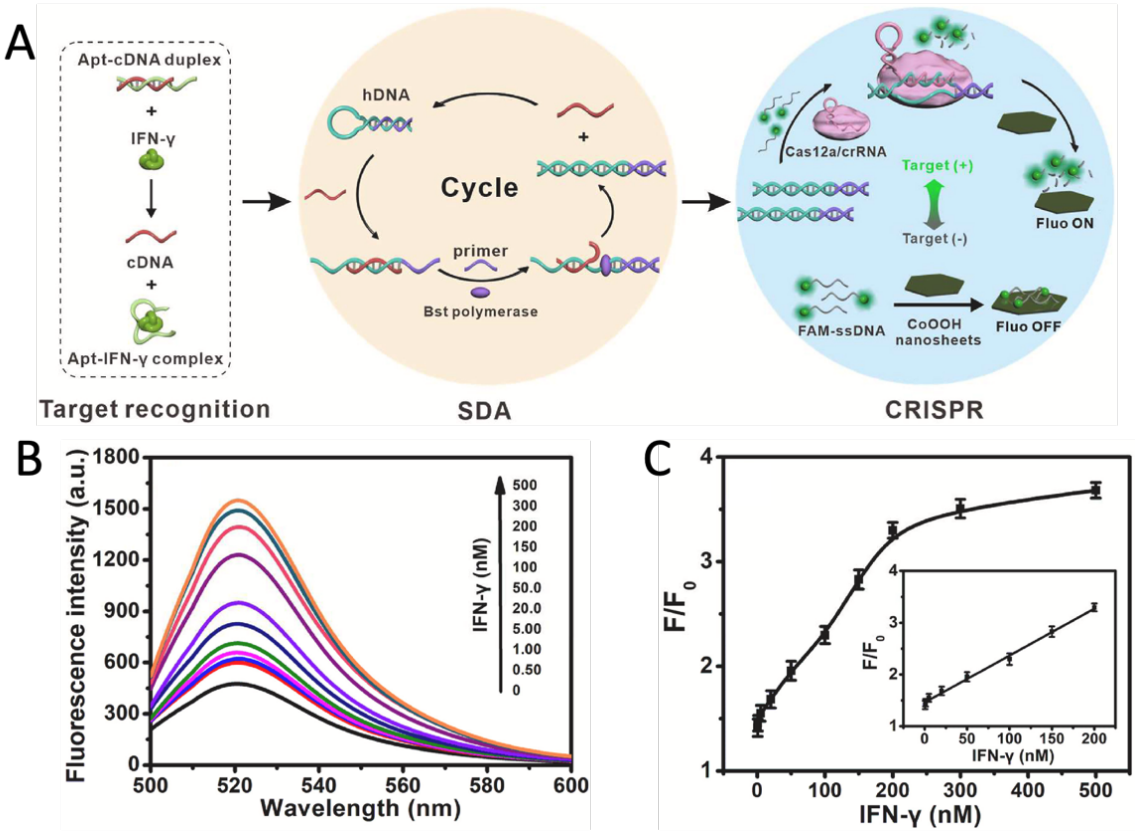

Figure 6. Apt-SCN strategy for IFN-γ detection. (**A**) Apt-SCN tandem scheme. (**B**) Changes in fluorescence spectra of Apt-SCN tandem method with increasing IFN-γ concentration (0-500 nM). (**C**) Correlation between the fluorescence intensity ratio F/F_0 and the IFN-γ concentration from Apt-SCN tandem system. Inset shows the calibration curve. Reproduced with permission.[71] Copyright 2023, Elsevier B.V.

fluorescence recovery and a signal conversion from 'off' to 'on' in response to IFN-γ. The Apt-SCN tandem method achieved a LOD of 0.37 nM IFN-γ (**Figure 6B** and **6C**), facilitated by CoOOH nanosheets favouring the adsorption of ssDNA, and reducing the need for costly quencher modifications. The collateral cleavage activity of CRISPR/Cas12a has also been leveraged for the detection of IFN-γ through the CAMERA platform (CRISPR/Cas and aptamer-mediated extra-sensitive assay).[72] Initially, an analyte recognition complex was prepared by mixing a fluorescence-labelled ssDNA aptamer with biotinylated cDNA, creating a dsDNA complex attached to a streptavidin-coated 96-well plate. In the presence of IFN-γ, the aptamer binds to the dsDNA complex, causing dissociation from the sensing interface. Subsequently, CRISPR/Cas12a RNPs were activated by the remaining aptamers, cleaving quenched fluorescent reporters, and producing a fluorescent signal. The signal intensity correlated with the remaining aptamer amount, which decreased as more analytes bound to the surface. The negative correlation between fluorescence intensity and analyte concentration yielded a sensitivity of 100 fg mL^{-1} IFN-γ in under

1.5 hours. Numerous quenching schemes exist, each tailored for specific applications. Notably, Fang et al. developed a photo-detachable DNA-copolymer nanocage on the T-cell membrane for the screening of cytokine secretion at the single-cell level.[73] The nanocage serves the critical function of confining locally secreted cytokines, such as IFN-γ, around the secreting cell during detection, thereby eliminating interference from nearby cells that may impair the single-cell distinguishing efficiency. Construction of the nanocage involved the interactions as seen in the scheme in **Figure 7A**. The detection DNA-copolymer and sealing DNA-copolymer were synthesized through the copolymerization of acrylamide and acrydite-modified DNA strands. The detection DNA-copolymer contains a self-quenched IFN-γ recognition aptamer. Upon secretion of IFN-γ, the self-quenched aptamer recovers its fluorescence indicating T-cell activity. The effectiveness of the system was successfully demonstrated for the monitoring of IFN-γ secretion at the single-cell level (**Figure 7B**). The subsequent selection of active T-cells using fluorescence-activated cell sorting (FACS) led to the detachment of the nanocage through UV irradiation. Sorted, active T-cells were continuously cocultured with Jurkat cells for improved functions in downstream cell activation and enhanced cancer cell killing (**Figure 7C**). For real-time monitoring of IFN-γ secretion, Jurkat cells were encapsulated with the DNA-copolymer nanocage. Upon stimulation with phorbol 12-myristate-13-acetate (PMA) and ionomycin, the Jurkat cells secreted IFN-γ, accompanied with even TAMRA fluorescence distribution on the cell membrane (**Figure 7D**), indicating successful nanocage assembly. With prolonged stimulation, some cells exhibited FAM fluorescence recovery, highlighting the nanocage's capability to screen IFN-γ secretion at the single-cell level for the subsequent FACS selection and downstream applications. Microfluidic techniques employing flow-assisted principles similar to FACS have also been exploited to facilitate compartmentalisation for IFN-γ detection, allowing precise management of biochemical reactions or single cells.[74, 75] Single-cell IFN-γ secretion was also detected using a quencher-free on-cell fluorescent aptamer labelled with BODIPY fluorophores.[76] On-cell detection of IFN-γ was demonstrated using BODIPY-labelled aptasensors immobilized on the cell membrane of T-lymphoblasts albeit with apparent background fluorescence issues. Challenges related to low fluorescence on/off values were attributed to the interaction between the excited fluorophore and guanine bases, a sensing scheme not fully elucidated. These challenges, along with concerns related to the effects of biotin modification for cell membrane immobilization, must be considered for practical applications. Achieving high resolution and good signal-to-noise ratios is vital for practical implementations, particularly in live-cell imaging. Increasing the Stokes shift of

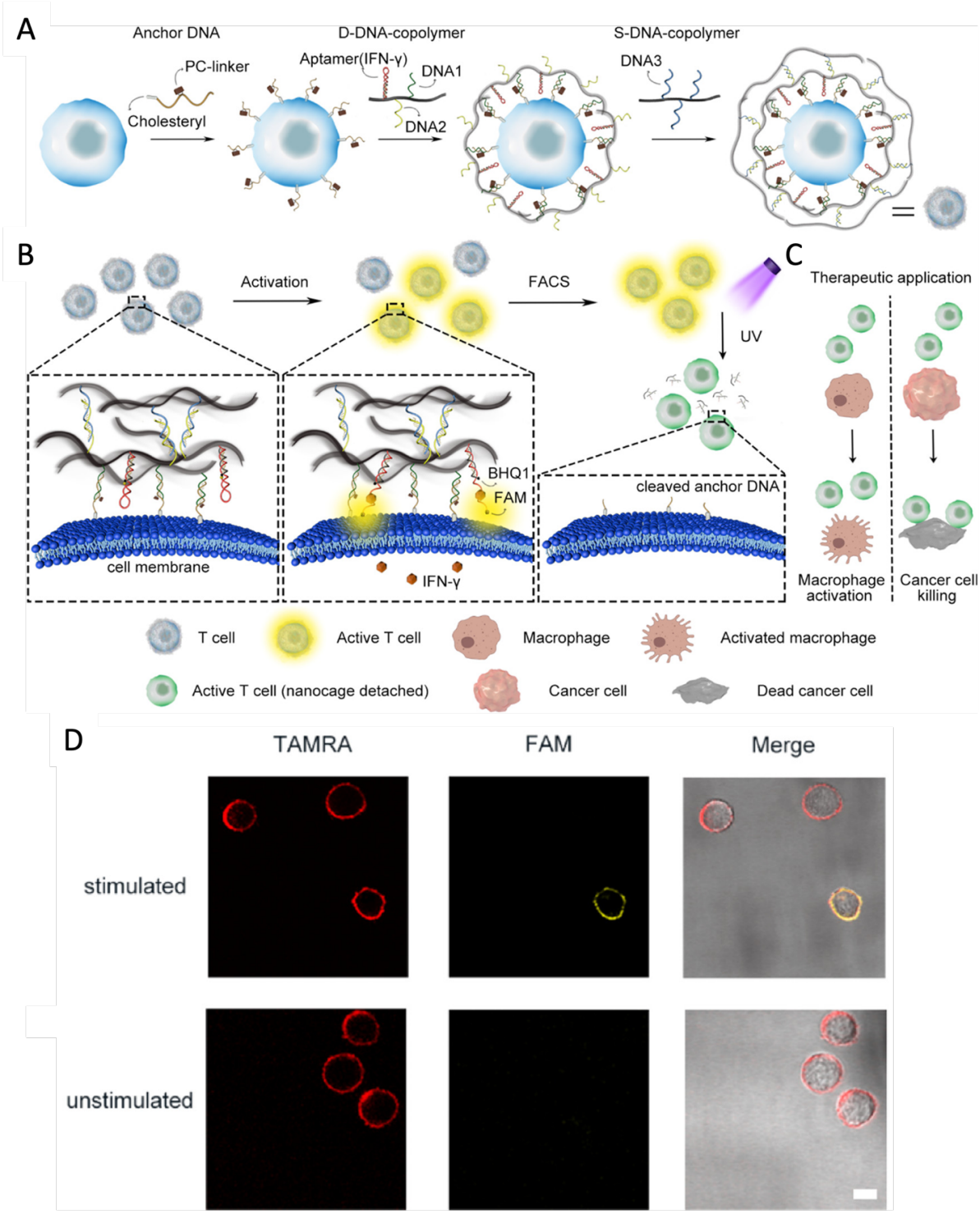

Figure 7. DNA-copolymer nanocage-encapsulated T cells for activity sorting. (**A**) Construction of detachable DNA-copolymer nanocage on the cell membrane. (**B**) Application in single-cell IFN-γ secretion detection for T-cell activity screening and selection and (**C**) detachment from the cell membrane for therapeutic usage. (**D**) Encapsulated DNA-copolymer nanocages-Jurkat cells with and without PMA and ionomycin stimulation. Scale bars: 10 μm. Reproduced with permission.[73] Copyright 2022, American Chemical Society.

BODIPY labels may reduce background fluorescence and enhance detectable changes, possibly leading to clearer distinctions in the low-range fluorescence intensities. Previous studies have successfully introduced vibronic structures and utilized through-bond energy transfer (TBET) cassettes to enhance the Stokes shift of fluorophore-complexes, while also demonstrating applicability in living cells.[77, 78] Moreover, mitigation of bulky biotin-streptavidin bio-conjugation might alleviate potential immunogenicity. For instance, a thiol-maleimide reaction was proposed for cell membrane conjugation, showing no adverse effects on cell viability, proliferation, or multipotency of stem cells, while offering controlled binding sites on the protein or peptides by strategically positioning free thiol-containing cysteine within these molecules.[79]

To facilitate simpler methods for point-of-care testing (POCT), some fluorescence-based sensors aim to minimise the complexities arising from disintegrated systems, quencher-pairs, and expensive assay requirements, such as enzyme-dependent biochemical reactions. To this end, enzyme-free detection schemes are being explored for cytokine detection. Qin et al. proposed a netlike hybridization chain reaction (nHCR) method to avoid the use of enzymes.[80] In their approach, IFN-γ binds to an aptamer hairpin probe, inducing a conformational change and releasing embedded nHCR initiator strands. These initiators unfold one of two double hairpin probes labelled with a FRET pair, initiating nHCR between them, forming a netlike DNA structure (**Figure 8A**). The resulting nHCR product amplifies FRET signals, leading to sensitive detection of IFN-γ at low picomolar levels (**Figure 8B** and **8C**). Nevertheless, the absence of enzymes can limit detection sensitivity, particularly preventing detection below picomolar levels, also evidenced by the enzyme-free approach presented by Cui et al.[81] Enzyme-based approaches provide the valuable exponential amplification as seen in techniques including Cas12a activity, SDA or loop-mediated isothermal amplification (LAMP)[82]. Achieving heightened sensitivities with HCR or other enzyme-free methods may necessitate interdisciplinary efforts. Notably, microRNA and mRNA detection has been accomplished by combining branched HCR or proximity-dependent surface HCR with electrochemiluminescence sensors, achieving LOD's of 0.18 fM and 3 fM, respectively.[83, 84]

The specific assay applications most often dictate which bioreceptor to choose. For instance, when prioritizing factors such as long-term durability and the need for extensive modifications to the receptor, the aptamer receptor emerges as the clear preference. Conversely, if the primary objectives include securing high-affinity binding and minimizing cross-reactivity, the antibody receptor is typically favoured. A recent advancement in highly sensitive protein detection scheme, known as Single-Molecule Recognition through Equilibrium Poisson Sampling (SiMREPS), has emerged as a powerful tool. While some reported applications of SiMREPS utilize antibodies as

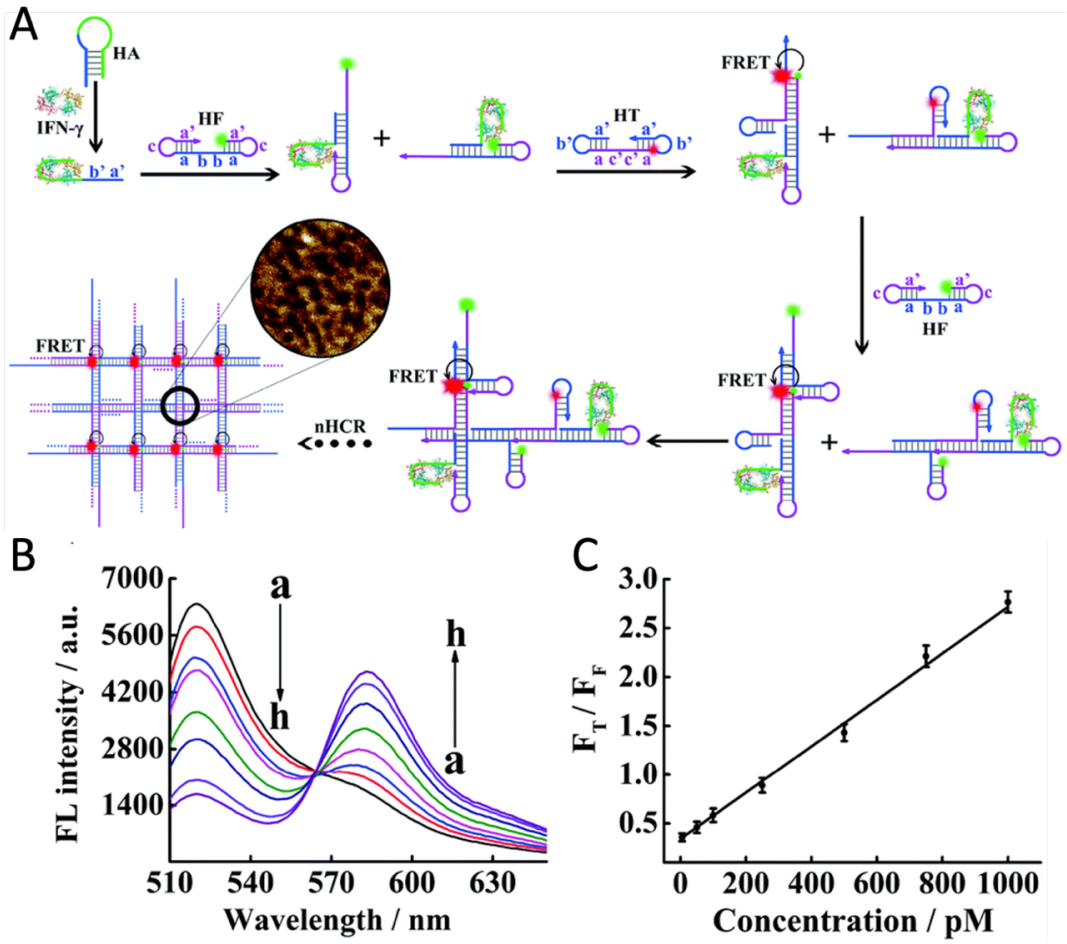

Figure 8. nHCR sensing strategy for IFN-γ. (**A**) nHCR scheme for enzyme-free and amplified IFN-γ detection. (**B**) nHCR DNA nanostructure fluorescence spectra for IFN-γ detection at different concentrations, [a] 0 pM to [h] 1000 pM. (**C**) Calibration plot of F_T/F_F ratio and concentration of IFN-γ from 5 pM to 1000 pM. Reproduced with permission.[80] Copyright 2019, Royal Society of Chemistry.

bioreceptors[85], this method capitalizes on binding and dissociation kinetics to differentiate signals originating from specific target binding from those resulting from non-specific interactions with the assay surface or matrix. Consequently, the assay exhibits a relaxed probe affinity requirement. Illustrated by Chatterjee et al., SiMREPS can employ fluorophore-labelled aptamers as detection probes for identifying proteins such as vascular endothelial growth factor 165 ($VEGF_{165}$, 38 kDa) and interleukin 8 (IL-8, 8.5 kDa) (**Figure 9A**).[86] Aptamer selection was guided by their amenability to rapid modification, facilitating fast dissociation kinetics for repeated interrogation of single target molecules without compromising sensitivity. Through subtle alterations in previously validated aptamer sequences against $VEGF_{165}$ and IL-8, such as single nucleotide substitutions or shortening of helical stems, modified aptamers were synthesized (**Figure 9B**). Optimization

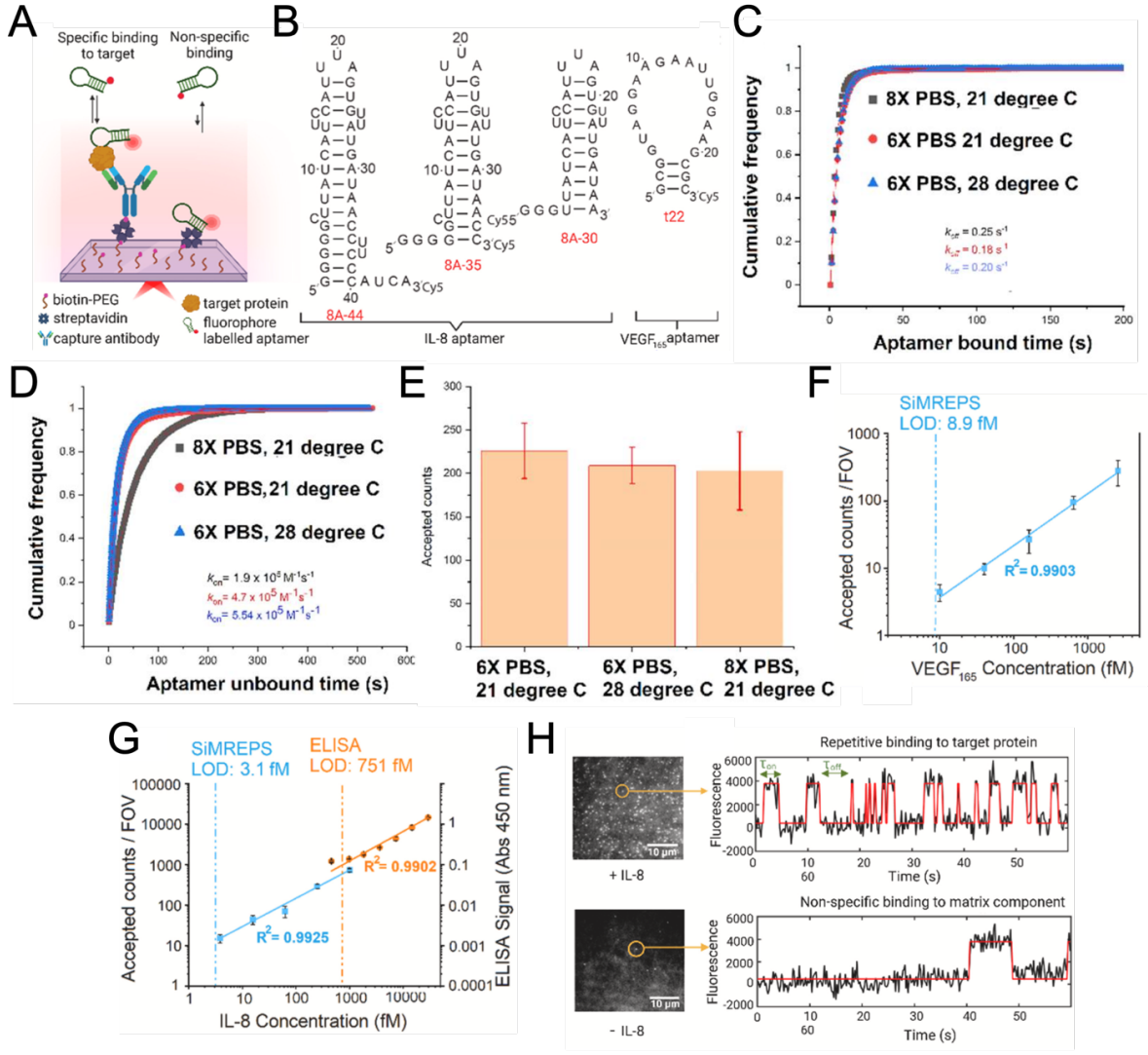

Figure 9. SiMREPS detection of $VEGF_{165}$ and IL-8. (**A**) Scheme aptamer-based SiMREPS cytokine detection. (**B**) Original sequences and secondary structures of IL-8 and $VEGF_{165}$ aptamers. Cumulative bound (**C**) and unbound (**D**) dwell time of Cy5-labelled $VEGF_{165}$ aptamer at different salt and temperature conditions. (**E**) Variation in accepted counts/field-of-view (VOF) for detection of 2.56 pM $VEGF_{165}$ by its modified aptamer. Standard curves of $VEGF_{165}$ (**F**) and IL-8 (**G**) quantification in spiked serum samples. (**H**) Movie frames of representative microscope FOV; bright points indicate single fluorophore-labelled aptamers bound to assay surface, and intensity-versus-time traces of distinct kinetic fingerprints of specific, repetitive binding (upper trace) and nonspecific binding (bottom trace). Reproduced with permission.[86] Copyright 2022, Elsevier B.V.

strategies to the aptamers included guanine-to-adenine base substitution for $VEGF_{165}$-specific aptamers and truncation of non-conserved aptamer portions for IL-8 specific ones. Moreover, regulating salt concentrations and temperature helped fine-tune kinetics (**Figure 9C-E**). These modifications culminated in achieving 8.9 fM (0.34 pg mL^{-1}) and 0.31 fM (0.026 pg mL^{-1}) LODs for $VEGF_{165}$ (**Figure 9F**) and IL-8 (**Figure 9G**), respectively, in spiked serum matrices, even without the need for washing steps. Remarkably, distinct kinetic interaction fingerprints associated

with non-specific binding of aptamers allowed facile discrimination from repetitive specific binding to the target protein. This phenomenon facilitated kinetic filtering, mitigating false positive counts while preserving true positives (**Figure 9H**). Evidently, the kinetics of the aptamer-analyte interaction hinges on numerous factors, including sequence length, base constituents, temperature, and ionic conditions, rendering the path to efficient SiMREPS rather complex. Nonetheless, the principle of SiMREPS is excellent for highlighting the significance of aptamer sequence modifications, as they ultimately dictate the nature of the target interaction.

Fluorescence-based aptasensors represent a promising avenue for sensitive and selective detection of cytokines, driven by innovative strategies such as specialized nanostructures, label-free sensing, and quenching strategies. While these sensors offer high sensitivities and diverse sensing mechanisms, their implementation often entails complex protocols requiring meticulous handling of components, which may limit their suitability for POCT. Moreover, the efficacy of reactions in fluorescence-based aptasensors is strongly influenced by environmental factors such as pH and ionic strength, complicating their transition to biological sample matrices. Thus, while offering considerable potential, further refinement is necessary to optimize the practical applicability of fluorescence-based aptasensors in diagnostic settings.

5. Colorimetric

Colorimetric biosensors offer a promising avenue for POC analyte detection due to their ease of fabrication, rapid detection, cost-effectiveness, and naked-eye measurement capability.[26] The emergence of nanomaterials, particularly AuNPs, has expanded opportunities within the field of colorimetric methods. Leveraging the unique plasmonic characteristics of AuNPs enables rapid aggregation and colour change in response to environmental alterations, forming the basis for aggregation plasmonic sensors.[87] In this context, colorimetric aptasensors, especially those utilizing nanomaterials such as AuNPs, hold potential for detecting cytokines.

Giorgi-Coll and co-workers developed a colorimetric aptasensor for IL-6 detection, employing AuNPs functionalized with a 'sandwich-pair' of aptamers.[25] This study marked the first application of such aptamers for IL-6 detection using AuNPs. The assay operates on the principle that IL-6 binding to multiple aptamers on the AuNP surface induces aggregation and result in a visible colour change, as shown in **Figure 10A**. Citrate-capped AuNPs (cAuNPs) were functionalized with thiolated aptamers specific to IL-6. A larger AuNP core size (50 nm) was found to enhance the assay response in terms of particle aggregation compared to smaller AuNP core sizes (15 nm). While effective in detecting IL-6 concentrations in the range of μg mL^{-1} (**Figure 10B** and **10C**), the assay demonstrated limitations in sensitivity for clinical relevance, suggesting the need for

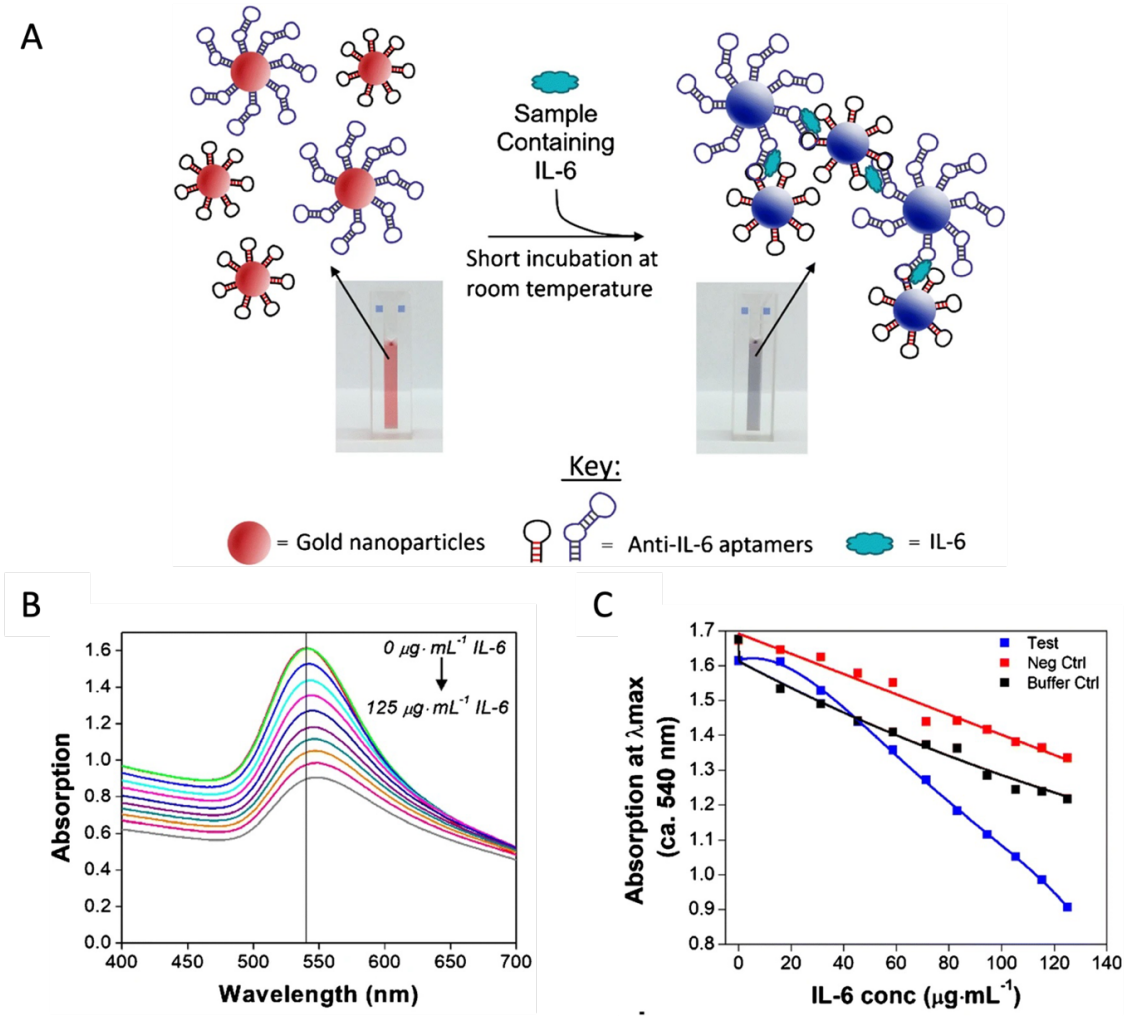

Figure 10. Aptamer-gold nanoparticle-based aggregation assay. (**A**) Schematic of sensing setup. (**B**) UV-Vis absorption spectra under different concentrations of IL-6. (**C**) Correlations between IL-6 concentration and absorption maxima. Reproduced with permission.[25] Copyright 2019, Giorgi-Coll, S. et al.

optimization strategies, including adjustment of aptamer-cAuNP concentrations and co-functionalization ratios. The assay, however, holds potential for clinical applications in a bedside 'dip-stick' format. Previously, certain aptamer-based colorimetric sensors have also utilized enzymatic amplification or enzyme-assisted cleavage of aptamer-complexes, achieving relatively low detection limits solely through colorimetric readouts.[88, 89]

Alternatively, Li and colleagues presented a robust dual-readout potential and colorimetric assay for IFN-γ detection in bodily fluids.[90] Their approach utilized an antifouling nanoparticle (ANP) and a gold nanoparticle (GNP) with cholesterol-labelled protein-responsive aptamers (**Figure 11A**). Upon IFN-γ introduction, aptamers underwent conformational changes, forming

core-shell nanostructures, and triggering an optical response in GNPs and amplified zeta potential. At low target concentrations, the zeta potential readout was reliable, whereas at higher concentrations, the colorimetric response was visible to the naked eye (**Figure 11B**). Various aptamer stem lengths were explored for stability enhancement (**Figure 11C**), revealing a 7 bp stem length as optimal for probe stability and sensitivity, and shorter stems (4-5 bp) producing a relatively high background signal and longer stems (10 bp) showing minimal response signal attributed to their high thermodynamically stable stem which inhibited the conformational switch of the DNA probe **(Figure 11D)**. This dual-readout strategy demonstrated a quasi-linear

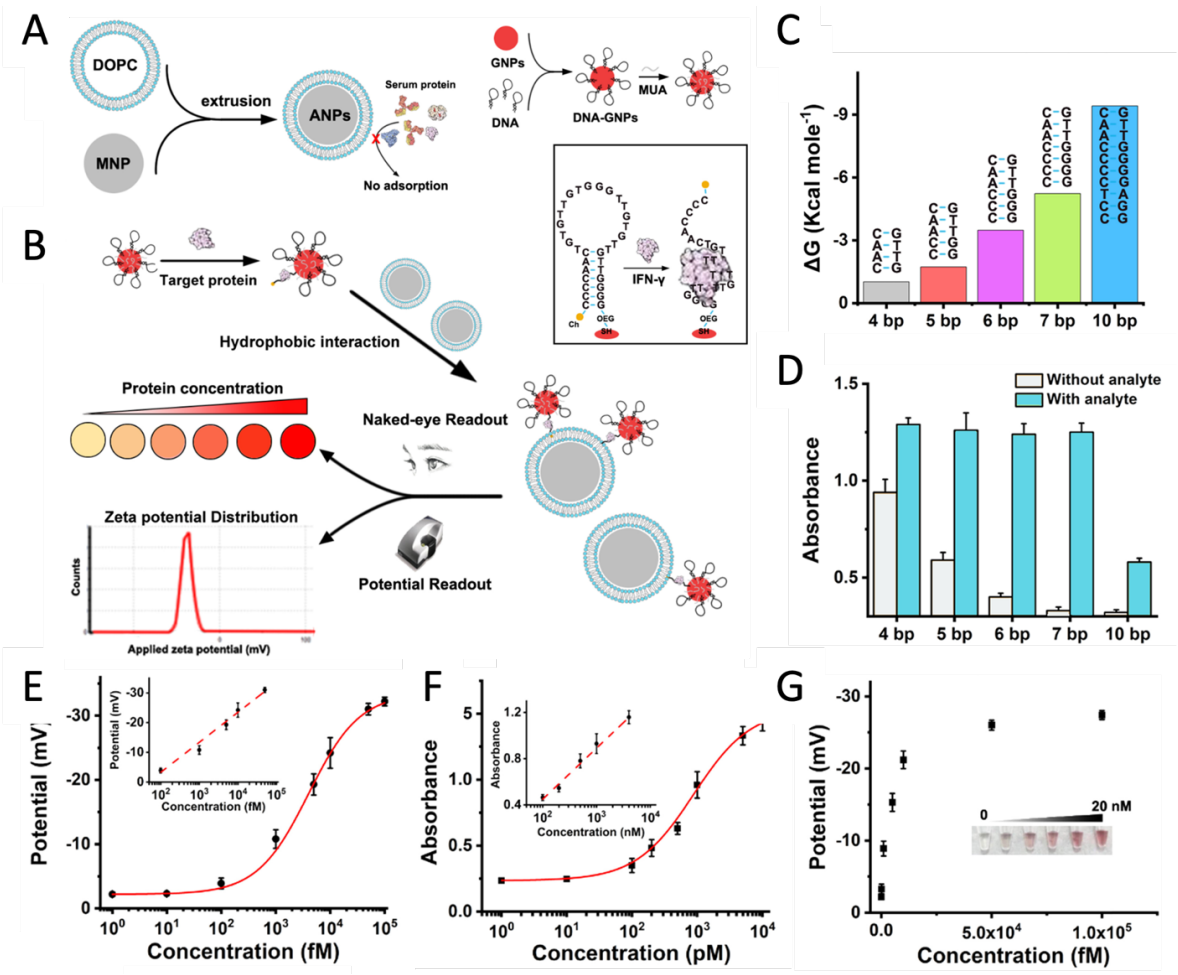

Figure 11. Dual-readout assay for detection of IFN-γ. (**A**) Sensing strategy involving two functional nanoparticles, ANPs and GNPs. (**B**) Scheme of dual-readout assay upon analyte introduction, with inset showing the aptamer configuration switch from IFN-γ recognition. (**C**) Various DNA strands of different stem lengths and their corresponding folding energy. (**D**) Response signal of ANPs after incubation with DNA-GNPs of different stem lengths with or without IFN-γ (10 nM). Analytical performance from (**E**) zeta potential and (**F**) colorimetric readout. (**G**) Detection of IFN-γ in spiked 10% fetal bovine serum, with inset showing the colorimetric responses to different IFN-γ concentrations (0, 0.5, 1, 5, 10, and 20 nM). Reproduced with permission.[90] Copyright 2021, Elsevier B.V.

relationship of potential intensity with IFN-γ concentration over wide range (**Figure 11E**), with a LOD of 78.8 fM. Colorimetric readout correlated well with IFN-γ concentrations from 0.1-5 nM, and a LOD of 38.8 pM (**Figure 11F**). Both readouts also produced noticeable changes when detecting IFN-γ in complex samples (**Figure 11G**). Compared to aggregation-based methods, Li et al.'s approach showcased highly enhanced detection limits, highlighting the importance of interdisciplinary efforts in sensor development.

Despite the limited availability of colorimetric aptasensors for cytokine detection, the incorporation of aggregation-induced signal change or a dual-readout strategy presents unique advantages to the field. While these methods demonstrate relatively high sensitivity and specificity, challenges such as aptamer specificity, assay complexity, and sensitivity limitations necessitate further exploration and optimization. Interdisciplinary collaboration is pivotal in advancing colorimetric sensing technologies, with significant strides made in developing tailored nanomaterials to improve signal transduction mechanisms. Despite this progress, there remains a noticeable gap in research focusing on diverse nanomaterials and enhanced POCT for aptamer-based colorimetric detection of cytokines. A range of nanomaterials, including metal oxide nanoparticles[91, 92], carbon materials[93], and MOFs[94], have been extensively utilized in biomedical applications due to their catalytic properties, resembling those of natural peroxidase enzymes.[26] In this context, a magnetic colorimetric immunoassay for IL-6 detection took advantage of the oxidase activity of ceria nanospheres. Substrate oxidation was catalysed by the ceria spheres producing a visible yellow product, achieving a LOD of 0.04 pg mL^{-1}.[95] Another approach utilized silver enhancement through nucleation on AuNPs in a lateral flow sensor to detect IL-6 via immunocomplexes with high sensitivity.[96] Lateral flow techniques, renowned for their simplicity, low cost, and rapid results, are commonly employed for enhanced POCT. Notably, some lateral flow aptasensors also employ amplification techniques such as HCR and recombinase polymerase amplification (RPA) to boost signals, diverging from traditional nanomaterials-based approaches.[97, 98]

Maintaining simple colorimetric readout techniques is crucial as signal enhancement methods become more complex. The advent of mobile densitometry apps for digital diagnostics presents a significant advantage for POCT by converting colorimetric signals into quantitative data using smartphones.[26] A recent example employed an aggregation-induced aptameric colorimetric sensor for the rapid detection of gliadin in food, a promising and highly convenient sensing technique for individuals with celiac disease.[99] Accuracy in smartphone analysis was achieved with a customized cassette designed to block internal random reflections, which otherwise hindered the colour-

picking process of the phone camera. The colorimetric signals could then be converted into RGB values, demonstrating a strong correlation across the range of 0.67-10 μM gliadin concentrations.

When addressing issues arising from lack of aptamer specificity, certain base modifications within the aptamer sequence have been shown to enhance the binding kinetics. For instance, slow-off rate modified aptamers (SOMAmers) were utilized for the inhibition of IL-6 signalling.[100] With the use of hydrophobic base substitutions of either 5-(N-benzylcarboxamide)-2'-deoxyuridine (Bn-dU) or 5-[N-(1-naphthylmethyl)carboxamide]-2'-deoxyuridine (Nap-dU) replacing dT bases in the aptamer sequences the aptamers exhibited exceptionally slow complex dissociation rates. Additionally, amino-modified pyrimidine residues in RNA aptamers and base substitutions can modulate aptamer specificity and affinity.[101, 102] Investigations into different spacers or linkers may also facilitate optimal aptamer structure switching upon analyte binding, ultimately leading to enhanced affinity and specificity, as explored by Tuleuova and her team in the design of a FRET-based aptamer beacon sensor against IFN-γ.[103] Exploring aptamer modifications in colorimetric sensors may help advance assay specificities and sensitivities in cytokine detection.

6. Chemiluminescent and other optical biosensors

Chemiluminescent aptasensors and liquid crystal (LC)-based biosensors represent significant advancements in biosensing technology, though less represented for the detection of cytokines. Chemiluminescence, characterized by light emission from a chemical reaction, offers notable advantages such as high sensitivity, low detection limits, wide linear dynamic ranges, simplicity, affordability, and rapid response.[104] These sensors, often employing biological enzymes or biomolecule-modified metallic nanoparticles for signal amplification, are gaining popularity, particularly when integrated with microchip electrophoresis to enhance sensitivity.[105] For instance, Yang et al. developed an ultrasensitive Microchip Electrophoresis-Chemiluminescence (MCE-CL) assay platform for detecting trace biomolecules associated with tuberculosis susceptibility, such as IFN-γ.[106] The platform, utilizing aptamers (P1) for target recognition and cyclic exonuclease cleavage technology for signal amplification (**Figure 12A**), achieved a remarkable seven-order-of-magnitude LOD (1.6 fM) compared to traditional MCE-CL methods, with a wide linear range from 8 fM to 10 nM (**Figure 12B**). Despite demonstrating specificity through interference testing with common proteins and successful application to human plasma samples, further validation with diverse targets, with greater similarity to IFN-γ, is necessary for broader disease diagnosis applicability (**Figure 12C**). A major setback for chemiluminescent methods is that they predominantly rely on labels for signal generation. In contrast, LCs offer intrinsic advantages for

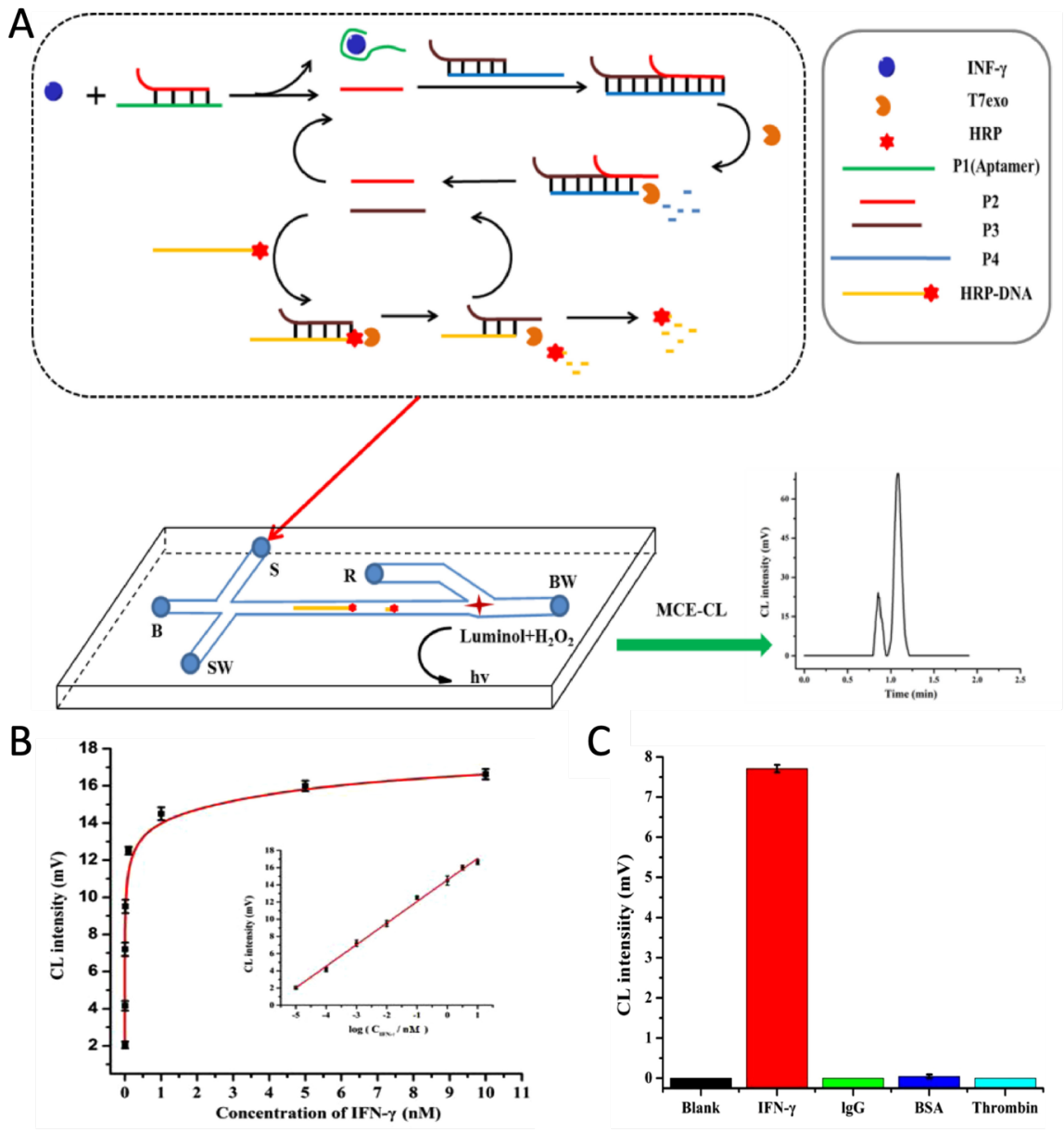

Figure 12. Chemiluminescent detection of IFN-γ. (**A**) Sensing principle of the MCE-CL platform based on IFN-γ triggering cascade CL signal amplification. (**B**) Correlation between IFN-γ concentration (10 fM to 10 nM) and the CL intensity obtained with MCE-CL assay. (**C**) Specificity of MCE-CL sensing for IFN-γ (1 pM) using BSA (0.1 nM), thrombin (0.1 nM), and IgG (1 ng mL^{-1}). Reproduced with permission.[106] Copyright 2019, Elsevier B.V.

sensitive label-free biomolecule detection, including signal amplification, surface sensitivity, and tailorable properties.[107] Kim and co-workers utilized the orientational behaviour of LCs in an aptasensor for IFN-γ detection, aiming at diagnosing latent tuberculosis (TB) using human blood samples.[108] Their sensor, based on the disruption of LC orientational order upon IFN-γ binding to

an aptamer-immobilized surface, achieved a LOD of 1 pM (17 pg mL^{-1}) with promising results in clinical tests. However, the limited number of clinical samples used necessitates further validation with a larger sample size for robust clinical applicability. Noteworthy advancements in aptameric LC biosensors, for non-cytokine targets, include the decoration of thin LC films with probe DNA and surfactants for multiplex detection of cancer biomarkers.[109] Additionally, novel developments involving aptamer structure switching to regulate the surface properties of orderly vertically aligned LCs upon analyte interaction have demonstrated promising potential for clinical analysis of bacterial endotoxins.[110] These innovations highlight the versatility and potential of aptameric LC-based biosensors, providing significant inspiration for developments in the field of cytokine detection and monitoring.

7. Conclusion

In summary, this review has provided a comprehensive exploration of cutting-edge optical aptasensors, encompassing plasmon-based setups (SPR, LSPR, SERS), fluorescence, chemiluminescent, and colorimetric assays tailored for cytokine detection. The persistent prevalence of inflammatory diseases underscores the imperative need for advanced sensing technologies. The optical aptasensors discussed herein exhibit exceptional sensitivities, boasting ultra-low detection limits, and expansive linear detection ranges, as detailed in **Table 1**. Noteworthy strategies, such as nanoparticle incorporation in LSPR and SERS, as well as enzyme-assisted amplification in select fluorescent aptasensor schemes, contribute to heightened assay sensitivity. Likewise, the specificity of the selected cytokine-specific aptamers underlines the potential for detecting trace amounts of cytokines in complex biological matrices. Yet, considering recent advancements, it is evident that many aptamer-based biosensing studies have yet to address certain critical aspects, such as the impact of immobilization and labelling on aptamer configuration and folding. For instance, fluorescence-based aptasensors typically rely on aptamer labelling which may influence the aptamer's specificity against its target. Moreover, when aptamers are surface immobilized in setups such as SERS, SPR, and colorimetric assays, steric hindrance may significantly affect the aptamer's ability to adopt its appropriate three-dimensional configuration required for target binding. Despite these challenges, aptamers hold considerable promise over antibodies due to their ease of modification and adaptability to different sensing scenarios. Continued research and development efforts aimed at overcoming these obstacles will further enhance the effectiveness and applicability of aptamer-based biosensing technologies for cytokines.

Table 1. Summary of optical aptasensors studied in this review.

Type	Strategy	Target	Linear range	LOD	Ref
SPR	Apt-Ab sandwich	TNF-α (17.4 kDa) NT-proBNP (8.5 kDa)	0.1-5 pM 0.05-0.5 nM	0.06 pM 0.03 nM	31
SPR	Dual apt, streptavidin	IFN-γ (17 kDa)	0.3-333 nM	0.03 nM	30
SPR	Dual apt, streptavidin	IFN-γ	0.01-100 nM	10 pM	34
LSPR	AuNRs, ADPA	IL-6 (20.9 kDa)	0.2 pM - 47.8 nM	0.2 pM	40
LSPR	AuNRs, competitive	IFN-γ	n/a	10 pM	42
SERS	AuNPs array, AAO	IL-6	0.1-100 nM	0.8 pM	24
SERS	AuNPs, self-calibration	IL-6	0.05 pM - 0.5 nM	2.7 fM	54
SERS	MNPs, Apt-Ab sandwich	TNF-α	0.1 fM - 0.57 nM	0.3 fM	55
Fluorescence	NCDs, AuNPs, FRET	IL-6	70-300 fM	40 fM	57
Fluorescence	GQD, aggregation, FRET	IFN-γ	0.29-5.9 pM	0.12 pM	58
Fluorescence	QD-aptamer-AuNP	TNF-α	0-22.3 nM	97.2 pM	59
Fluorescence	Iridium(III) probe	IFN-γ	1-100 nM	0.12 nM	60
Fluorescence	AIEgen, aggregation	IFN-γ	0-5.9 pM	0.12 pM	61
Fluorescence	MOFs	IFN-γ	0.06 fM - 6 pM	0.057 fM	62
Fluorescence	MM_{GO}	IL-6	3 fM - 47.8 pM	1 fM	63
Fluorescence	MM_{GO}, simultaneous	IL-6 PCT (14.5 kDa)	2.4 fM - 47.8 pM 0.7 pM - 8.8 nM	7.2 fM 0.2 pM	64
Fluorescence	rGO NS	IFN-γ	5.9 pM - 0.59 μM	5.9 pM	68
Fluorescence	GO NS	IFN-γ	3.5 fM - 1 pM	1.5 fM	69
Fluorescence	NS ReS_2/TiS_2, FRET	IFN-γ	0-400 pM (ReS_2) 0-300 pM (TiS_2)	57.6 pM (ReS_2) 82.7 pM (TiS_2)	70
Fluorescence	SDA, CRISPR/Cas12a	IFN-γ	0.5-200 nM	0.37 nM	71
Fluorescence	CRISPR/Cas12a	IFN-γ	5.9 fM - 0.59 nM	5.9 fM	72
Fluorescence	Nanocage, quencher	IFN-γ	n/a	n/a	73
Fluorecence	Microfluidics	IFN-γ	n/a	10 μM	74
Fluorescence	Microfluidics	IFN-γ	n/a	10 nM	75
Fluorescence	BODIPY, on-cell	IFN-γ	n/a	n/a	76
Fluorescence	nHCR	IFN-γ	5-1000 pM	1.2 pM	80
Fluorescence	CHA, amplification	IFN-γ	0.05-1000 pM	0.047 pM	81
Fluorescence	LAMP	IFN-γ	0.3-4.7 nM	0.14 nM	82
Fluorescence	SiMREPS	$VEGF_{165}$ (38 kDa) IL-8 (8.5 kDa)	n/a	8.9 fM 3.1 fM	86

Fluorescence	FRET	IFN-γ	5-100 nM	5 nM	103
Colorimetric	AuNPs, aggregation	IL-6	0.16-6 μM	93.3 nM	25
Colorimetric	Quadratic amplification	IFN-γ	0-100 nM	1.5 pM	88
Colorimetric	Strand-cleavage	IFN-γ	n/a	0.1 pM	89
Colorimetric	Dual readout	IFN-γ	100 fM - 50 pM	78.8 pM	90
Chemiluminescence	AuNP, G-quadruplex	IFN-γ	0.5-100 nM	0.4 nM	105
Chemiluminescence	MCE-CL, CSA	IFN-γ	8 fM - 10 nM	1.6 fM	106
Liquid crystal	Orientational disruption	IFN-γ	n/a	1 pM	108

Abbreviations: AAO, anodic aluminium oxide; Ab, antibody; ADPA, antibody-derived peptide aptamer; AIEgen, aggregation-induced emission; Apt, aptamer; AuNP, gold nanoparticle; AuNR, gold nanorod; CHA, catalytic hairpin assembly; CSA, cascade signal amplification; FRET, Förster resonance energy transfer; GO, graphene oxide; IFN-γ, interferon-gamma; IL-6, interleukin-6; IL-8, interleukin-8; LAMP, loop-mediated isothermal amplification; MCE-CL, Microchip Electrophoresis-Chemiluminescence; MM_{GO}, graphene oxide/nickel/platinum nanoparticle micromotor; MNP, magnetic nanoparticle; MOF, metallic organic framework; NCD, nitrogen-doped carbon quantum dots; nHCR, netlike hybridization chain reaction; NS, nanosheet; NT-proBNP, N-terminal prohormone of brain natriuretic peptide; PCT, procalcitonin; QD, quantum dot; rGO, reduced graphene oxide; SDA, strand displacement amplification; SiMREPS, single-molecule recognition through equilibrium Poisson sampling; TNF-α, tumor necrosis factor-alpha; VEGF, vascular endothelial growth factor.

Acknowledgements

This work is supported under the UTT Project Stratégique NanoSPR (OPE-2022-0293), the Graduate School (Ecole Universitaire de Recherche) "NANOPHOT" (ANR-18-EURE-0013), and PHC PROCORE-Campus France/Hong Kong Joint Research Scheme (No. 44683Q). The authors also would like to acknowledge the support provided by the Research Grants Council of the Hong Kong Special Administrative Region, China (project #: CUHK 14207121), the VC Discretionary Fund provided by the Chinese University of Hong Kong (project #: 8601014), the State Key Laboratory of Marine Pollution (SKLMP) Seed Collaborative Research Fund (project #: SKLMP/SCRF/0042) provided by the City University of Hong Kong and the PhD International Mobility for Partnerships and Collaborations (PhD IMPAC) Award granted by the Chinese University of Hong Kong.

Received: ((will be filled in by the editorial staff))
Revised: ((will be filled in by the editorial staff))
Published online: ((will be filled in by the editorial staff))

References

(1) Stenken, J. A.; Poschenrieder, A. J. Bioanalytical chemistry of cytokines--a review. *Anal Chim Acta* **2015**, *853*, 95-115. DOI: 10.1016/j.aca.2014.10.009 From NLM Medline.

(2) O'Shea, J. J.; Gadina, M.; Kanno, Y. Cytokine signaling: birth of a pathway. *J Immunol* **2011**, *187* (11), 5475-5478. DOI: 10.4049/jimmunol.1102913 From NLM Medline.

(3) Huang, K. J.; Su, I. J.; Theron, M.; Wu, Y. C.; Lai, S. K.; Liu, C. C.; Lei, H. Y. An interferon-gamma-related cytokine storm in SARS patients. *J Med Virol* **2005**, *75* (2), 185-194. DOI: 10.1002/jmv.20255 From NLM Medline.

(4) Mehta, P.; McAuley, D. F.; Brown, M.; Sanchez, E.; Tattersall, R. S.; Manson, J. J.; Hlh Across Speciality Collaboration, U. K. COVID-19: consider cytokine storm syndromes and immunosuppression. *Lancet* **2020**, *395* (10229), 1033-1034. DOI: 10.1016/S0140-6736(20)30628-0 From NLM Medline.

(5) Jarczak, D.; Nierhaus, A. Cytokine Storm-Definition, Causes, and Implications. *Int J Mol Sci* **2022**, *23* (19). DOI: 10.3390/ijms231911740 From NLM Medline.

(6) Qudus, M. S.; Tian, M.; Sirajuddin, S.; Liu, S.; Afaq, U.; Wali, M.; Liu, J.; Pan, P.; Luo, Z.; Zhang, Q.; et al. The roles of critical pro-inflammatory cytokines in the drive of cytokine storm during SARS-CoV-2 infection. *J Med Virol* **2023**, *95* (4), e28751. DOI: 10.1002/jmv.28751 From NLM Medline.

(7) Landskron, G.; De la Fuente, M.; Thuwajit, P.; Thuwajit, C.; Hermoso, M. A. Chronic inflammation and cytokines in the tumor microenvironment. *J Immunol Res* **2014**, *2014*, 149185. DOI: 10.1155/2014/149185 From NLM Medline.

(8) Boshtam, M.; Asgary, S.; Kouhpayeh, S.; Shariati, L.; Khanahmad, H. Aptamers Against Pro- and Anti-Inflammatory Cytokines: A Review. *Inflammation* **2017**, *40* (1), 340-349. DOI: 10.1007/s10753-016-0477-1 From NLM Medline.

(9) Baker, K. J.; Houston, A.; Brint, E. IL-1 Family Members in Cancer; Two Sides to Every Story. *Front Immunol* **2019**, *10*, 1197. DOI: 10.3389/fimmu.2019.01197 From NLM Medline.

(10) Liu, C.; Chu, D.; Kalantar-Zadeh, K.; George, J.; Young, H. A.; Liu, G. Cytokines: From Clinical Significance to Quantification. *Adv Sci (Weinh)* **2021**, *8* (15), e2004433. DOI: 10.1002/advs.202004433 From NLM Medline.

(11) Song, S.; Wang, L.; Li, J.; Fan, C.; Zhao, J. Aptamer-based biosensors. *TrAC Trends in Analytical Chemistry* **2008**, *27* (2), 108-117. DOI: 10.1016/j.trac.2007.12.004.

(12) Iliuk, A. B.; Hu, L.; Tao, W. A. Aptamer in bioanalytical applications. *Anal Chem* **2011**, *83* (12), 4440-4452. DOI: 10.1021/ac201057w From NLM Medline.

(13) Tan, W.; Zhao, Z.; Zhang, L. APTAMER PROPERTIES, FUNCTIONS, AND APPLICATIONS. In *Nucleic Acids in Medicinal Chemistry and Chemical Biology*, 2023; pp 443-482.

(14) Tuerk, C.; Gold, L. Systematic evolution of ligands by exponential enrichment: RNA ligands to bacteriophage T4 DNA polymerase. *Science* **1990**, *249* (4968), 505-510. DOI: 10.1126/science.2200121 From NLM Medline.

(15) Kohlberger, M.; Gadermaier, G. SELEX: Critical factors and optimization strategies for successful aptamer selection. *Biotechnol Appl Biochem* **2022**, *69* (5), 1771-1792. DOI: 10.1002/bab.2244 From NLM Medline.

(16) Gold, L. SELEX: How It Happened and Where It will Go. *J Mol Evol* **2015**, *81* (5-6), 140-143. DOI: 10.1007/s00239-015-9705-9 From NLM Medline.

(17) Mashayekhi, K.; Ganji, A.; Sankian, M. Designing a new dimerized anti human TNF-alpha aptamer with blocking activity. *Biotechnol Prog* **2020**, *36* (4), e2969. DOI: 10.1002/btpr.2969 From NLM Medline.

(18) Billet, B.; Chovelon, B.; Fiore, E.; Oukacine, F.; Petrillo, M. A.; Faure, P.; Ravelet, C.; Peyrin, E. Aptamer Switches Regulated by Post-Transition/Transition Metal Ions. *Angew Chem Int Ed Engl* **2021**, *60* (22), 12346-12350. DOI: 10.1002/anie.202102254 From NLM PubMed-not-MEDLINE.

(19) Xu, M.; Peng, Y.; Yang, H.; Zhou, Y. Highly sensitive biosensor based on aptamer and hybridization chain reaction for detection of cadmium ions. *Luminescence* **2022**, *37* (4), 665-671. DOI: 10.1002/bio.4207 From NLM Medline.

(20) Alkhamis, O.; Canoura, J.; Bukhryakov, K. V.; Tarifa, A.; DeCaprio, A. P.; Xiao, Y. DNA Aptamer-Cyanine Complexes as Generic Colorimetric Small-Molecule Sensors. *Angew Chem Int Ed Engl* **2022**, *61* (3), e202112305. DOI: 10.1002/anie.202112305 From NLM PubMed-not-MEDLINE.

(21) Hariri, A. A.; Cartwright, A. P.; Dory, C.; Gidi, Y.; Yee, S.; Thompson, I. A. P.; Fu, K. X.; Yang, K.; Wu, D.; Maganzini, N.; et al. Modular Aptamer Switches for the Continuous Optical Detection of Small-Molecule Analytes in Complex Media. *Adv Mater* **2023**, e2304410. DOI: 10.1002/adma.202304410 From NLM Publisher.

(22) Ngoc Tran, B.; Thanh Pham, H.; Ngoc Pham, M. T.; Anh Nguyen, H. T.; Nguyen, Q. D.; Nguyen, H. T.; Tu, M. B.; Pham, B. Uncovering Adenosine-Specific Signals: A Label-Free Aptamer-Based Approach with Gold Nanoparticles for Specific Detection. *ChemistrySelect* **2023**, *8* (27). DOI: 10.1002/slct.202302282.

(23) Kim, J.; Noh, S.; Park, J. A.; Park, S. C.; Park, S. J.; Lee, J. H.; Ahn, J. H.; Lee, T. Recent Advances in Aptasensor for Cytokine Detection: A Review. *Sensors* **2021**, *21* (24). DOI: 10.3390/s21248491 From NLM Medline.

(24) Muhammad, M.; Shao, C.-s.; Huang, Q. Aptamer-functionalized Au nanoparticles array as the effective SERS biosensor for label-free detection of interleukin-6 in serum. *Sensors and Actuators B: Chemical* **2021**, *334*. DOI: 10.1016/j.snb.2021.129607.

(25) Giorgi-Coll, S.; Marin, M. J.; Sule, O.; Hutchinson, P. J.; Carpenter, K. L. H. Aptamer-modified gold nanoparticles for rapid aggregation-based detection of inflammation: an optical assay for interleukin-6. *Microchimica Acta* **2019**, *187* (1), 13. DOI: 10.1007/s00604-019-3975-7 From NLM Medline.

(26) Majdinasab, M.; Lamy de la Chapelle, M.; Marty, J. L. Recent Progresses in Optical Biosensors for Interleukin 6 Detection. *Biosensors* **2023**, *13* (9). DOI: 10.3390/bios13090898 From NLM Publisher.

(27) Chang, C. C. Recent Advancements in Aptamer-Based Surface Plasmon Resonance Biosensing Strategies. *Biosensors* **2021**, *11* (7). DOI: 10.3390/bios11070233 From NLM Medline.

(28) Wang, Z.; Wilkop, T.; Xu, D.; Dong, Y.; Ma, G.; Cheng, Q. Surface plasmon resonance imaging for affinity analysis of aptamer-protein interactions with PDMS microfluidic chips. *Anal Bioanal Chem* **2007**, *389* (3), 819-825. DOI: 10.1007/s00216-007-1510-x From NLM Medline.

(29) Wang, J.; Munir, A.; Zhu, Z.; Zhou, H. S. Magnetic nanoparticle enhanced surface plasmon resonance sensing and its application for the ultrasensitive detection of magnetic nanoparticle-enriched small molecules. *Anal Chem* **2010**, *82* (16), 6782-6789. DOI: 10.1021/ac100812c From NLM Medline.

(30) Chang, C. C.; Lin, S.; Lee, C. H.; Chuang, T. L.; Hsueh, P. R.; Lai, H. C.; Lin, C. W. Amplified surface plasmon resonance immunosensor for interferon-gamma based on a streptavidin-incorporated aptamer. *Biosens Bioelectron* **2012**, *37* (1), 68-74. DOI: 10.1016/j.bios.2012.04.038 From NLM Medline.

(31) Lee, S. H.; Back, J. H.; Joo, H. J.; Lim, D. S.; Lee, J. E.; Lee, H. J. Simultaneous detection method for two cardiac disease protein biomarkers on a single chip modified with mixed aptamers using surface plasmon resonance. *Talanta* **2024**, *267*, 125232. DOI: 10.1016/j.talanta.2023.125232 From NLM Medline.

(32) MacDonald, H.; Bonnet, H.; Van der Heyden, A.; Defrancq, E.; Spinelli, N.; Coche-Guérente, L.; Dejeu, J. Influence of Aptamer Surface Coverage on Small Target Recognition: A SPR and QCM-D Comparative Study. *Journal of Physical Chemistry* **2019**, *123*, 13561-13568.

(33) Simon, L.; Bognár, Z.; Gyurscányi, R. E. Finding the Optimal Surface Density of Aptamer Monolayers by SPR Imaging Detection-based Aptamer Microarrays. *Electroanalysis* **2020**, *32*, 851-858.

(34) Chuang, T. L.; Chang, C. C.; Chu-Su, Y.; Wei, S. C.; Zhao, X. H.; Hsueh, P. R.; Lin, C. W. Disposable surface plasmon resonance aptasensor with membrane-based sample handling design for quantitative interferon-gamma detection. *Lab Chip* **2014**, *14* (16), 2968-2977. DOI: 10.1039/c4lc00249k From NLM Medline.

(35) Kim, S.; Wark, A. W.; Lee, H. J. Femtomolar Detection of Tau Proteins in Undiluted Plasma Using Surface Plasmon Resonance. *Anal Chem* **2016**, *88* (15), 7793-7799. DOI: 10.1021/acs.analchem.6b01825 From NLM Medline.

(36) Duanghathaipornsuk, S.; Reaver, N. G. F.; Cameron, B. D.; Kim, D. S. Adsorption Kinetics of Glycated Hemoglobin on Aptamer Microarrays with Antifouling Surface Modification. *Langmuir* **2021**, *37* (15), 4647-4657. DOI: 10.1021/acs.langmuir.1c00446 From NLM Medline.

(37) Wang, Y.; Zeng, S.; Crunteanu, A.; Xie, Z.; Humbert, G.; Ma, L.; Wei, Y.; Brunel, A.; Bessette, B.; Orlianges, J. C.; et al. Targeted Sub-Attomole Cancer Biomarker Detection Based on Phase Singularity 2D Nanomaterial-Enhanced Plasmonic Biosensor. *Nanomicro Lett* **2021**, *13* (1), 96. DOI: 10.1007/s40820-021-00613-7 From NLM PubMed-not-MEDLINE.

(38) Zhu, S.; Jaffiol, R.; Crunteanu, A.; Vezy, C.; Chan, S. T.; Yuan, W.; Ho, H. P.; Zeng, S. Label-free biosensing with singular-phase-enhanced lateral position shift based on atomically thin plasmonic nanomaterials. *Light Sci Appl* **2024**, *13* (1), 2. DOI: 10.1038/s41377-023-01345-6 From NLM PubMed-not-MEDLINE.

(39) Chiu, N. F.; Kuo, C. T.; Chen, C. Y. High-affinity carboxyl-graphene oxide-based SPR aptasensor for the detection of hCG protein in clinical serum samples. *Int J Nanomedicine* **2019**, *14*, 4833-4847. DOI: 10.2147/IJN.S208292 From NLM Medline.

(40) He, J.; Zhou, L.; Huang, G.; Shen, J.; Chen, W.; Wang, C.; Kim, A.; Zhang, Z.; Cheng, W.; Dai, S.; et al. Enhanced Label-Free Nanoplasmonic Cytokine Detection in SARS-CoV-2 Induced Inflammation Using Rationally Designed Peptide Aptamer. *ACS Appl Mater Interfaces* **2022**, *14* (43), 48464-48475. DOI: 10.1021/acsami.2c14748 From NLM Medline.

(41) Ramezani, F.; Amanlou, M.; Rafii-Tabar, H. Comparison of amino acids interaction with gold nanoparticle. *Amino Acids* **2014**, *46* (4), 911-920. DOI: 10.1007/s00726-013-1642-6 From NLM Medline.

(42) Lin, D. Z.; Chuang, P. C.; Liao, P. C.; Chen, J. P.; Chen, Y. F. Increasing the spectral shifts in LSPR biosensing using DNA-functionalized gold nanorods in a competitive assay format for the

detection of interferon-gamma. *Biosens Bioelectron* **2016**, *81*, 221-228. DOI: 10.1016/j.bios.2016.02.071 From NLM Medline.

(43) Jain, P. K.; El-Sayed, M. A. Plasmonic coupling in noble metal nanostructures. *Chemical Physics Letters* **2010**, *487* (4-6), 153-164. DOI: 10.1016/j.cplett.2010.01.062.

(44) Hall, W. P.; Ngatia, S. N.; Van Duyne, R. P. LSPR Biosensor Signal Enhancement Using Nanoparticle-Antibody Conjugates. *J Phys Chem C Nanomater Interfaces* **2011**, *115* (5), 1410-1414. DOI: 10.1021/jp106912p From NLM PubMed-not-MEDLINE.

(45) Spadavecchia, J.; Barras, A.; Lyskawa, J.; Woisel, P.; Laure, W.; Pradier, C. M.; Boukherroub, R.; Szunerits, S. Approach for plasmonic based DNA sensing: amplification of the wavelength shift and simultaneous detection of the plasmon modes of gold nanostructures. *Anal Chem* **2013**, *85* (6), 3288-3296. DOI: 10.1021/ac3036316 From NLM Medline.

(46) Balamurugan, S.; Obubuafo, A.; McCarley, R. L.; Soper, S. A.; Spivak, D. A. Effect of linker structure on surface density of aptamer monolayers and their corresponding protein binding efficiency. *Anal Chem* **2008**, *80* (24), 9630-9634. DOI: 10.1021/ac8009559 From NLM Medline.

(47) de Mol, N. J.; Dekker, F. J.; Broutin, I.; Fischer, M. J.; Liskamp, R. M. Surface plasmon resonance thermodynamic and kinetic analysis as a strategic tool in drug design. Distinct ways for phosphopeptides to plug into Src- and Grb2 SH2 domains. *J Med Chem* **2005**, *48* (3), 753-763. DOI: 10.1021/jm049359e From NLM Medline.

(48) Xu, H.; Bjerneld, E. J.; Käll, M.; Börjesson, L. Spectroscopy of Single Hemoglobin Molecules by Surface Enhanced Raman Scattering

. *Physical Review Letters* **1999**, *83* (21), 4357-4360.

(49) Etchegoin, P.; Maher, R. C.; Cohen, L. F.; Hartigan, H.; Brown, R. J. C.; Milton, M. J. T.; Gallop, J. C. New limits in ultrasensitive trace detection by surface enhanced Raman scattering (SERS). *Chemical Physics Letters* **2003**, *375* (1-2), 84-90. DOI: 10.1016/s0009-2614(03)00821-2.

(50) Zhang, Y.; Wang, Z.; Wu, L.; Zong, S.; Yun, B.; Cui, Y. Combining Multiplex SERS Nanovectors and Multivariate Analysis for In Situ Profiling of Circulating Tumor Cell Phenotype Using a Microfluidic Chip. *Small* **2018**, *14* (20), e1704433. DOI: 10.1002/smll.201704433 From NLM Medline.

(51) Wang, D.; Wang, F.; Yang, H. Robust, flexible, sticky and high sensitive SERS membrane for rapid detection applications. *Sensors and Actuators B: Chemical* **2018**, *274*, 676-681. DOI: 10.1016/j.snb.2018.07.113.

(52) Rhinehardt, K. L.; Vance, S. A.; Mohan, R. V.; Sandros, M.; Srinivas, G. Molecular modeling and SPRi investigations of interleukin 6 (IL6) protein and DNA aptamers. *J Biomol Struct Dyn* **2018**, *36* (8), 1934-1947. DOI: 10.1080/07391102.2017.1338619 From NLM Medline.

(53) Majdinasab, M.; Azziz, A.; Liu, Q.; Mora-Sanz, V.; Briz, N.; Edely, M.; Lamy de la Chapellea, M. Label-free SERS for rapid identification of interleukin 6 based on intrinsic SERS fingerprint of antibody-gold nanoparticles conjugate. *Int J Biol Macromol* **2023**, *253* (Pt 8), 127560. DOI: 10.1016/j.ijbiomac.2023.127560 From NLM Medline.

(54) Huang, Q.; Chen, X.; Fan, M.; Ruan, S.; Peng, S.; You, R.; Chen, J.; Lu, Y. SERS-based self-calibrating aptamer sensor for selective detection of IL-6. *Sensors and Actuators B: Chemical* **2023**, *374*. DOI: 10.1016/j.snb.2022.132828.

(55) Nie, Q.; Zhang, B.; Li, R.; Yang, Y.; Ren, J.; Qiu, J.; Lu, Y.; Zhu, L.; Shen, H.; Liu, Y.; et al. Ultra-sensitive detection of tumor necrosis factor alpha based on silver-coated gold core shell and magnetically separated recognition of SERS aptamer sensors. *Microchimica Acta* **2024**, *191*.

(56) Ilyas, A.; Dyussupova, A.; Sultangaziyev, A.; Shevchenko, Y.; Filchakova, O.; Bukasov, R. SERS immuno- and apta-assays in biosensing/bio-detection: Performance comparison, clinical applications, challenges. *Talanta* **2023**, *265*, 124818. DOI: 10.1016/j.talanta.2023.124818 From NLM Publisher.

(57) Mahani, M.; Faghihi-Fard, M.; Divsar, F.; Torkzadeh-Mahani, M.; Khakbaz, F. Ultrasensitive FRET-based aptasensor for interleukin-6 as a biomarker for COVID-19 progression using nitrogen-doped carbon quantum dots and gold nanoparticles. *Microchimica Acta* **2022**, *189* (12), 472. DOI: 10.1007/s00604-022-05570-5 From NLM Medline.

(58) Liu, G.; Zhang, K.; Ma, K.; Care, A.; Hutchinson, M. R.; Goldys, E. M. Graphene quantum dot based "switch-on" nanosensors for intracellular cytokine monitoring. *Nanoscale* **2017**, *9* (15), 4934-4943. DOI: 10.1039/c6nr09381g From NLM Medline.

(59) Ghosh, S.; Datta, D.; Chaudhry, S.; Dutta, M.; Stroscio, M. A. Rapid Detection of Tumor Necrosis Factor-Alpha Using Quantum Dot-Based Optical Aptasensor. *IEEE Trans Nanobioscience* **2018**, *17* (4), 417-423. DOI: 10.1109/TNB.2018.2852261 From NLM Medline.

(60) Lin, S.; He, B.; Yang, C.; Leung, C. H.; Mergny, J. L.; Ma, D. L. Luminescence switch-on assay of interferon-gamma using a G-quadruplex-selective iridium(III) complex. *Chem Commun* **2015**, *51* (89), 16033-16036. DOI: 10.1039/c5cc06655g From NLM Medline.

(61) Ma, K.; Zhang, F.; Sayyadi, N.; Chen, W.; Anwer, A. G.; Care, A.; Xu, B.; Tian, W.; Goldys, E. M.; Liu, G. "Turn-on" Fluorescent Aptasensor Based on AIEgen Labeling for the Localization of IFN-gamma in Live Cells. *ACS Sens* **2018**, *3* (2), 320-326. DOI: 10.1021/acssensors.7b00720 From NLM Medline.

(62) Xia, J.; Bo, B.; Yang, S.; Cao, Y.; Cao, Y.; Cui, H. Interfacial reactivity-modulated fluorescent metal-organic frameworks for sensitive detection of interferon-gamma towards tuberculosis diagnosis. *Microchimica Acta* **2023**, *191* (1), 6. DOI: 10.1007/s00604-023-06088-0 From NLM Medline.

(63) Gordón, J.; Arruza, L.; Ibanez, M. D.; Moreno-Guzman, M.; Lopez, M. A.; Escarpa, A. On the Move-Sensitive Fluorescent Aptassay on Board Catalytic Micromotors for the Determination of Interleukin-6 in Ultra-Low Serum Volumes for Neonatal Sepsis Diagnostics. *ACS Sens* **2022**, *7* (10), 3144-3152. DOI: 10.1021/acssensors.2c01635 From NLM Medline.

(64) Gordón Pidal, J. M.; Arruza, L.; Moreno-Guzmán, M.; López, M. Á.; Escarpa, A. Micromotor-based dual aptassay for early cost-effective diagnosis of neonatal sepsis. *Microchimica Acta* **2024**, *191*, 106.

(65) Cai, L.; Xu, D.; Zhang, Z.; Li, N.; Zhao, Y. Tailoring Functional Micromotors for Sensing. *Research (Wash D C)* **2023**, *6*, 0044. DOI: 10.34133/research.0044 From NLM PubMed-not-MEDLINE.

(66) Wang, D. X.; Wang, Y. X.; Wang, J.; Ma, J. Y.; Liu, B.; Tang, A. N.; Kong, D. M. MnO2 nanosheets as a carrier and accelerator for improved live-cell biosensing application of CRISPR/Cas12a. *Chem. Sci.* **2022**, *13*, 4364-4371.

(67) Lv, Y.; Sun, Y.; Khan, I. M.; Li, Q.; Zhou, Y.; Yue, L.; Zhang, Y.; Wang, Z. Locking-DNA network regulated CRISPR-Cas12a fluorescent aptasensor based on hollow flower-like magnetic MoS2 microspheres for sensitive detection of sulfadimethoxine. *Chemical Engineering Journal* **2023**, *459*, 141463.

(68) Kim, M. G.; Shon, Y.; Lee, J.; Byun, Y.; Choi, B. S.; Kim, Y. B.; Oh, Y. K. Double stranded aptamer-anchored reduced graphene oxide as target-specific nano detector. *Biomaterials* **2014**, *35* (9), 2999-3004. DOI: 10.1016/j.biomaterials.2013.12.058 From NLM Medline.

(69) Hu, K.; Liu, J.; Chen, J.; Huang, Y.; Zhao, S.; Tian, J.; Zhang, G. An amplified graphene oxide-based fluorescence aptasensor based on target-triggered aptamer hairpin switch and strand-displacement polymerization recycling for bioassays. *Biosens Bioelectron* **2013**, *42*, 598-602. DOI: 10.1016/j.bios.2012.11.025 From NLM Medline.

(70) Dhenadhayalan, N.; Sriram, M. I.; Lin, K.-C. Aptamer-based fluorogenic sensing of interferon-gamma probed with ReS2 and TiS2 nanosheets. *Sensors and Actuators B: Chemical* **2018**, *258*, 929-936. DOI: 10.1016/j.snb.2017.11.178.

(71) Ren, D.; Chen, Q.; Xia, X.; Xu, G.; Wei, F.; Yang, J.; Hu, Q.; Cen, Y. CRISPR/Cas12a-based fluorescence aptasensor integrated with two-dimensional cobalt oxyhydroxide nanosheets for IFN-

gamma detection. *Anal Chim Acta* **2023**, *1278*, 341750. DOI: 10.1016/j.aca.2023.341750 From NLM Medline.

(72) Li, Y.; Liu, L.; Qiao, L.; Deng, F. Universal CRISPR/Cas12a-associated aptasensor suitable for rapid detection of small proteins with a plate reader. *Front Bioeng Biotechnol* **2023**, *11*, 1201175. DOI: 10.3389/fbioe.2023.1201175 From NLM PubMed-not-MEDLINE.

(73) Fang, Y.; Yan, Y.; Bi, S.; Wang, Y.; Chen, Y.; Xu, P.; Ju, H.; Liu, Y. Screening T-Cell Activity via a Photodetachable DNA-Copolymer Nanocage and Its Therapeutic Application. *Anal Chem* **2022**, *94* (38), 13205-13214. DOI: 10.1021/acs.analchem.2c02763 From NLM Medline.

(74) Sochol, R. D.; Corbett, D.; Hesse, S.; Krieger, W. E.; Wolf, K. T.; Kim, M.; Iwai, K.; Li, S.; Lee, L. P.; Lin, L. Dual-mode hydrodynamic railing and arraying of microparticles for multi-stage signal detection in continuous flow biochemical microprocessors. *Lab Chip* **2014**, *14* (8), 1405-1409. DOI: 10.1039/c4lc00012a From NLM Medline.

(75) Qiu, L.; Wimmers, F.; Weiden, J.; Heus, H. A.; Tel, J.; Figdor, C. G. A membrane-anchored aptamer sensor for probing IFNgamma secretion by single cells. *Chem Commun* **2017**, *53* (57), 8066-8069. DOI: 10.1039/c7cc03576d From NLM Medline.

(76) Tsuchiya, A.; Hashim, S. N.; Ise, S.; Furuhata, T.; Kawai, K.; Wakabayashi, R.; Goto, M.; Kamiya, N.; Sando, S. BODIPY-labeled Fluorescent Aptamer Sensors for Turn-on Sensing of Interferon-gamma and Adenine Compounds on Cells. *Anal Sci* **2016**, *32* (5), 543-547. DOI: 10.2116/analsci.32.543 From NLM Medline.

(77) Ren, T. B.; Xu, W.; Zhang, W.; Zhang, X. X.; Wang, Z. Y.; Xiang, Z.; Yuan, L.; Zhang, X. B. A General Method To Increase Stokes Shift by Introducing Alternating Vibronic Structures. *J Am Chem Soc* **2018**, *140* (24), 7716-7722. DOI: 10.1021/jacs.8b04404 From NLM PubMed-not-MEDLINE.

(78) Qu, X.; Liu, Q.; Ji, X.; Chen, H.; Zhou, Z.; Shen, Z. Enhancing the Stokes' shift of BODIPY dyes via through-bond energy transfer and its application for Fe(3+)-detection in live cell imaging. *Chem Commun* **2012**, *48* (38), 4600-4602. DOI: 10.1039/c2cc31011b From NLM Medline.

(79) Li, P. Y.; Fan, Z.; Cheng, H. Cell Membrane Bioconjugation and Membrane-Derived Nanomaterials for Immunotherapy. *Bioconjug Chem* **2018**, *29* (3), 624-634. DOI: 10.1021/acs.bioconjchem.7b00669 From NLM Medline.

(80) Qin, Y.; Li, D.; Yuan, R.; Xiang, Y. Netlike hybridization chain reaction assembly of DNA nanostructures enables exceptional signal amplification for sensing trace cytokines. *Nanoscale* **2019**, *11* (35), 16362-16367. DOI: 10.1039/c9nr04988f From NLM Medline.

(81) Cui, H.; Bo, B.; Ma, J.; Tang, Y.; Zhao, J.; Xiao, H. A target-responsive liposome activated by catalytic hairpin assembly enables highly sensitive detection of tuberculosis-related cytokine. *Chem Commun* **2018**, *54* (38), 4870-4873. DOI: 10.1039/c8cc01542b From NLM Medline.

(82) Chen, W.; Fang, X.; Ye, X.; Li, H.; Cao, H.; Kong, J. DNA nanomachine-assisted magnetic bead based target recycling and isothermal amplification for sensitive fluorescence determination of interferon-γ. *Microchimica Acta* **2017**, *184* (12), 4869-4877. DOI: 10.1007/s00604-017-2511-x.

(83) Li, Y.; Huang, C. Z.; Li, Y. F. Ultrasensitive Electrochemiluminescence Detection of MicroRNA via One-Step Introduction of a Target-Triggered Branched Hybridization Chain Reaction Circuit. *Anal Chem* **2019**, *91* (14), 9308-9314. DOI: 10.1021/acs.analchem.9b02580 From NLM Medline.

(84) Cheng, Y. H.; Liu, S. J.; Jiang, J. H. Enzyme-free electrochemical biosensor based on amplification of proximity-dependent surface hybridization chain reaction for ultrasensitive mRNA detection. *Talanta* **2021**, *222*, 121536. DOI: 10.1016/j.talanta.2020.121536 From NLM Medline.

(85) Chatterjee, T.; Knappik, A.; Sandford, E.; Tewari, M.; Choi, S. W.; Strong, W. B.; Thrush, E. P.; Oh, K. J.; Liu, N.; Walter, N. G.; et al. Direct kinetic fingerprinting and digital counting of single protein molecules. *Proc Natl Acad Sci U S A* **2020**, *117* (37), 22815-22822. DOI: 10.1073/pnas.2008312117 From NLM Medline.

(86) Chatterjee, T.; Johnson-Buck, A.; Walter, N. G. Highly sensitive protein detection by aptamer-based single-molecule kinetic fingerprinting. *Biosens Bioelectron* **2022**, *216*, 114639. DOI: 10.1016/j.bios.2022.114639 From NLM Medline.

(87) Yang, J.; Wang, X.; Sun, Y.; Chen, B.; Hu, F.; Guo, C.; Yang, T. Recent Advances in Colorimetric Sensors Based on Gold Nanoparticles for Pathogen Detection. *Biosensors* **2023**, *13* (1). DOI: 10.3390/bios13010029 From NLM Medline.

(88) Zhou, W.; Gong, X.; Xiang, Y.; Yuan, R.; Chai, Y. Target-triggered quadratic amplification for label-free and sensitive visual detection of cytokines based on hairpin aptamer DNAzyme probes. *Anal Chem* **2014**, *86* (1), 953-958. DOI: 10.1021/ac403682c From NLM Medline.

(89) Zhang, K.; Ren, T.; Wang, K.; Zhu, X.; Wu, H.; Xie, M. Sensitive and selective amplified visual detection of cytokines based on exonuclease III-aided target recycling. *Chem Commun* **2014**, *50* (87), 13342-13345. DOI: 10.1039/c4cc05701e From NLM Medline.

(90) Li, C.; Wang, F.; Liu, T.; Yang, Y. A highly sensitive, dual-readout assay based on self-assembly of two functional nanoparticles for homogeneous detection of protein biomarkers. *Sensors and Actuators B: Chemical* **2021**, *348*, 130710.

(91) Gao, L.; Zhuang, J.; Nie, L.; Zhang, J.; Zhang, Y.; Gu, N.; Wang, T.; Feng, J.; Yang, D.; Perrett, S.; et al. Intrinsic peroxidase-like activity of ferromagnetic nanoparticles. *Nat Nanotechnol* **2007**, *2* (9), 577-583. DOI: 10.1038/nnano.2007.260 From NLM Medline.

(92) Huang, Y.; Zhong, H.; Jiang, C.; Yang, J.; Zhang, J.; Zhao, F.; Liu, C. Copper-based nanomaterials as peroxidase candidates for intelligent colorimetric detection and antibacterial applications. *Particuology* **2024**, *84*, 126-135.

(93) Sun, H.; Zhou, Y.; Ren, J.; Qu, X. Carbon Nanozymes: Enzymatic Properties, Catalytic Mechanism, and Applications. *Angew Chem Int Ed Engl* **2018**, *57* (30), 9224-9237. DOI: 10.1002/anie.201712469 From NLM Medline.

(94) Nath, I.; Chakraborty, J.; Verpoort, F. Metal organic frameworks mimicking natural enzymes: a structural and functional analogy. *Chem Soc Rev* **2016**, *45* (15), 4127-4170. DOI: 10.1039/c6cs00047a From NLM Medline.

(95) Peng, J.; Guan, J.; Yao, H.; Jin, X. Magnetic colorimetric immunoassay for human interleukin-6 based on the oxidase activity of ceria spheres. *Anal Biochem* **2016**, *492*, 63-68. DOI: 10.1016/j.ab.2015.09.018 From NLM Medline.

(96) Rahbar, M.; Wu, Y.; Subramony, J. A.; Liu, G. Sensitive Colorimetric Detection of Interleukin-6 via Lateral Flow Assay Incorporated Silver Amplification Method. *Front Bioeng Biotechnol* **2021**, *9*, 778269. DOI: 10.3389/fbioe.2021.778269 From NLM PubMed-not-MEDLINE.

(97) Ying, N.; Wang, Y.; Song, X.; Yang, L.; Qin, B.; Wu, Y.; Fang, W. Lateral flow colorimetric biosensor for detection of Vibrio parahaemolyticus based on hybridization chain reaction and aptamer. *Microchimica Acta* **2021**, *188* (11), 381. DOI: 10.1007/s00604-021-05031-5 From NLM Medline.

(98) Du, Y.; Liu, D.; Wang, M.; Guo, F.; Lin, J. S. Preparation of DNA aptamer and development of lateral flow aptasensor combining recombinase polymerase amplification for detection of erythromycin. *Biosens Bioelectron* **2021**, *181*, 113157. DOI: 10.1016/j.bios.2021.113157 From NLM Medline.

(99) Qin, Y.; Zhang, S.; Qian, J.; Meng, F.; Yao, J.; Zhang, M. Lable-free aptamer portable colorimetric smartphone for gliadin detection in food. *Front Bioeng Biotechnol* **2024**, *12*, 1338408. DOI: 10.3389/fbioe.2024.1338408 From NLM PubMed-not-MEDLINE.

(100) Gupta, S.; Hirota, M.; Waugh, S. M.; Murakami, I.; Suzuki, T.; Muraguchi, M.; Shibamori, M.; Ishikawa, Y.; Jarvis, T. C.; Carter, J. D.; et al. Chemically modified DNA aptamers bind interleukin-6 with high affinity and inhibit signaling by blocking its interaction with interleukin-6

receptor. *J Biol Chem* **2014**, *289* (12), 8706-8719. DOI: 10.1074/jbc.M113.532580 From NLM Medline.

(101) Kubik, M. F.; Bell, C.; Fitzwater, T.; Watson, S. R.; Tasset, D. M. Isolation and characterization of 2'-fluoro-, 2'-amino-, and 2'-fluoro-/amino-modified RNA ligands to human IFN-gamma that inhibit receptor binding. *J Immunol* **1997**, *159* (1), 259-267. From NLM Medline.

(102) Manuel, B. A.; Sterling, S. A.; Sanford, A. A.; Heemstra, J. M. Systematically Modulating Aptamer Affinity and Specificity by Guanosine-to-Inosine Substitution. *Anal Chem* **2022**, *94* (17), 6436-6440. DOI: 10.1021/acs.analchem.2c00422 From NLM Medline.

(103) Tuleuova, N.; Jones, C. N.; Yan, J.; Ramanculov, E.; Yokobayashi, Y.; Revzin, A. Development of an aptamer beacon for detection of interferon-gamma. *Anal Chem* **2010**, *82* (5), 1851-1857. DOI: 10.1021/ac9025237 From NLM Medline.

(104) Sun, Y.; Lu, J. Chemiluminescence-based aptasensors for various target analytes. *Luminescence* **2018**, *33* (8), 1298-1305. DOI: 10.1002/bio.3557 From NLM Medline.

(105) Jiang, J.; He, Y.; Yu, X.; Zhao, J.; Cui, H. A homogeneous hemin/G-quadruplex DNAzyme based turn-on chemiluminescence aptasensor for interferon-gamma detection via in-situ assembly of luminol functionalized gold nanoparticles, deoxyribonucleic acid, interferon-gamma and hemin. *Anal Chim Acta* **2013**, *791*, 60-64. DOI: 10.1016/j.aca.2013.06.048 From NLM Medline.

(106) Yang, X.; Zhao, J.; Chen, S.; Huang, Y.; Zhaok, S. An ultrasensitive microchip electrophoresis chemiluminescence assay platform for detection of trace biomolecules. *J Chromatogr A* **2020**, *1613*, 460693. DOI: 10.1016/j.chroma.2019.460693 From NLM Medline.

(107) Wang, H.; Xu, T.; Fu, Y.; Wang, Z.; Leeson, M. S.; Jiang, J.; Liu, T. Liquid Crystal Biosensors: Principles, Structure and Applications. *Biosensors* **2022**, *12* (8). DOI: 10.3390/bios12080639 From NLM Medline.

(108) Kim, H. J.; Jang, C.-H. Liquid crystal-based aptasensor for the detection of interferon-γ and its application in the diagnosis of tuberculosis using human blood. *Sensors and Actuators B: Chemical* **2019**, *282*, 574-579. DOI: 10.1016/j.snb.2018.11.104.

(109) Qi, L.; Hu, Q.; Kang, Q.; Bi, Y.; Jiang, Y.; Yu, L. Detection of Biomarkers in Blood Using Liquid Crystals Assisted with Aptamer-Target Recognition Triggered in Situ Rolling Circle Amplification on Magnetic Beads. *Anal Chem* **2019**, *91* (18), 11653-11660. DOI: 10.1021/acs.analchem.9b02186 From NLM Medline.

(110) An, Z.; Jang, C.-H. Simple and Label-Free Liquid Crystal-based Optical Sensor for Highly Sensitive and Selective Endotoxin Detection by Aptamer Binding and Separation. *ChemistrySelect* **2019**, *4*, 1416-1422.